often is a reflection of earlier patterning defects. For instance, the *baltan* mutant shows severe degeneration in the forebrain and has an early patterning defect (Kitagawa et al., 2004).

2.4.2. Early PGC mutants

Many mutations affecting the distribution and/or abundance of PGCs at st. 26 were identified (Sasado et al., 2004). Mutations in 10 genes caused an altered distribution of PGCs, affecting PGC migration, accumulation and redistribution. The majority of mutant phenotypes in this class were associated with other morphological abnormalities, suggesting that the mutated gene is involved in various aspects of organogenesis. All of the mutations that reduced the number of PGCs exerted their effects only when the mother was a heterozygous carrier, indicating the contribution of maternal factors to the determination of PGC abundance.

2.4.3. Later-stage germ cell mutants

Screening of germ cells for *vasa* expression was also carried out at the larval stage when the sex of an animal can be distinguished by the abundance of *vasa*-positive germ cells. The female gonad is large and asymmetric and the male gonad is smaller and symmetric, as shown in Fig. 3.

The proliferation and/or distribution of germ cells during gonadal development was affected in mutants corresponding to 13 genes (Morinaga et al., 2004). Three mutations caused an increase in the number of germ cells. One interesting mutation, *totoro*, caused the tumorous growth of immature germ cells in homozygous juvenile adults. In other mutants, the abnormal distribution of germ cell clusters was accompanied by an irregular gonad shape, suggesting an interaction between germ cells and non-germ line gonadal anlage in gonadal development.

2.4.4. Lateral line mutants

The lateral line system is a sensory organ found in fish and amphibians. The posterior lateral line nerve (PLLn) shows stereotyped projections from the hindbrain to the neuromasts, groups of cells receiving sensory stimuli in the trunk. Mutations in four genes were isolated that affected the PLLn trajectory. Among the mutations identified, *kazura* (*kaz*) and *yanagi* (*yan*) mutations displayed specific defects in projection of the posterior lateral line nerve. The *yan* and *kaz* mutants also exhibited defects in the migration of primordial germ cells.

2.4.5. Mutants affecting liver development and function

Mutations in 19 genes affected the liver at various stages of development (Watanabe et al., 2004). These mutations were classified into five phenotypic groups in terms of liver morphogenesis, laterality, bile color, lipid metabolism and endoderm formation. Mutations in the first group, *kakurenbo*, *hiogi*, and *origami*, affect the size of the liver as well as the morphology of the gall bladder and gut, suggesting that these genes are involved in gut endoderm development.

2.4.6. Thymus mutants

Cells derived from three germ layers, neural crest cells from the ectoderm, lymphocytes from the mesoderm and cells of the thymic anlage from the endodermal pharyngeal pouch are thought to contribute to thymus organogenesis (Manley, 2000; Jenkinson et al., 2003; Bennett et al., 2002; Gill et al., 2002). Using *rag1* (*recombination activating gene 1*) expression in thymocytes as a marker of thymus development, we isolated 24 mutations defining at least 13 genes (Iwanami et al., 2004). Several mutants showed a range of defects in the pharyngeal arches from which the thymus anlagen develops. Thus, the primary defect may reside in the thymus anlage, leading to the failure of thymus formation. Other mutants with defective *rag1* expression showed normal pharyngeal arch development, suggesting that the mutations disrupt colonizing lymphocytes.

2.4.7. Eye mutants

The Kyoto screen together with previous morphological screens identified 60 mutations that affect retinal development (Loosli et al., 2004). The mutants were grouped into five classes: 11 mutants were affected in neural plate and optic vesicle formation, 15 mutants showed impaired growth of optic vesicles, 18 mutants were defective in optic cup development, 13 mutants showed abnormal retinal differentiation, 12 of which had small eyes and one caused enlarged eyes, and three mutants had abnormal retinal pigmentation.

2.4.8. Retino-tectal mutants

In Medaka, as in other lower vertebrates, the axons of RGCs project to the visual center of the brain, the optic tectum. To project the image on the retina precisely, all the RGC axons connect to the opposite side (contralateral) of the tectum, preserving the topological relationship with different points on the retina. Mutations in five genes affecting the projections of RGC axons to the retina were identified (Yoda et al., 2004). The misrouting of RGC axons occurred either between the retina and chiasm (Group 1 mutants) or between the chiasm and the tectum (Group 2 mutants). While misrouted axons reached the tectum on the same side (ipsilateral) of the retina in Group 1 mutants, misrouted axons did not project to the tectum in Group 2 mutants. Defects appear to be restricted to RGC axons in contrast to previously described zebrafish mutants (Karlstrom et al., 1996), as other tissues appear unaffected in the Medaka mutants.

2.4.9. Somitogenesis mutants

Mutations in nine genes affected somite formation and mutants were classified into two groups (Elmasri et al., 2004). Group 1 mutations caused phenotypes characterized by the complete or partial absence of somites or somite boundaries and Group 2 mutations resulted in fused somites or somites of irregular size and shape. The majority of

the mutants exhibited somitic phenotypes, such as individually fused somites and irregular somite sizes, that were distinct from those found in zebrafish (van Eeden et al., 1996). Three mutations were also isolated that produced characteristic phenotypes similar to those of zebrafish mutations affecting the Delta/Notch signaling pathway (van Eeden et al., 1996).

2.4.10. γ-Ray sensitivity mutants

A new type of screen was modified for fish to recover mutants that exhibit increased sensitivity to γ-ray radiation during development (Aizawa et al., 2004). After irradiation of F3 embryos using a dose at which wild-type embryos readily recover from damage, mutants were obtained by screening for whole-embryo viability. Three genes termed *ric* (radiation-induced curly tailed) *1–3* were identified in this screen. The *ric1* mutation was found to affect the repair of double-stranded DNA breaks induced by γ-ray, suggesting a DNA surveillance function for the *ric1* gene product during early embryogenesis (Aizawa et al., 2004).

3. Discussion

We have summarized the characteristics of developmental mutants collected in the first large-scale systematic screen carried out in Medaka in which multiple phenotypic traits were assayed. We observed much commonality between Medaka and zebrafish mutants, as may be expected, but also significant differences in the phenotypic spectrum between the two fish species. This finding validates the use of two complementary fish model systems for mutational analyses to probe developmental and cellular processes.

From a practical point of view, the visibility of a particular tissue during inspection of an embryo is an important factor in determining the ease of mutant identification. In a Medaka embryo, internal organs such as the liver and gall bladder are more conspicuous than those in zebrafish, while the notochord and melanophores are not as easily assayed. The types of mutants isolated in zebrafish and Medaka screens indeed reflect this difference in ease of tissue visualization (Haffter et al., 1996; Driever et al., 1996).

3.1. Distinct phenotypes between Medaka and zebrafish

The similarity in embryogenesis between Medaka and zebrafish allows the comparison and correspondence of developmental stages, morphogenetic landmarks, and hence mutant phenotypes. An important observation is that mutations in Medaka cause unique phenotypes that have so far not been described for zebrafish. For example, many Medaka mutations that affect forebrain development cause novel phenotypes that do not have an obvious correspondence to those of zebrafish mutants (Kitagawa et al., 2004).

The extent and timing of functional overlap among related genes may be sufficiently different to produce different sets of mutant phenotypes between the two fish models. Alternatively, regulation of forebrain development may involve divergent genetic pathways in the two species. Another formal possibility is that the susceptibility of some genetic loci to mutagenesis is substantially different between Medaka and zebrafish. In any event, the distinct phenotypes of the recovered mutants underscore the value of studying Medaka and zebrafish in parallel.

3.2. Phenotypes shared by Medaka and zebrafish mutants

Several Medaka mutants show a high degree of phenotypic similarity to zebrafish mutants. Recovered mutants with specific defects (Kitagawa et al., 2004; Watanabe et al., 2004) exhibited phenotypes resembling those of zebrafish *bozozok*, *one-eyed-pinhead*, *cyclops*, *masterblind*, *no isthmus*, *acerebellar*, *no tail* and *spadetail* mutants (Haffter et al., 1996; Driever et al., 1996).

A shared phenotype does not necessarily indicate that exactly the same set of genes or signals operate in the two fishes. Thus, even when the mutant phenotype is very similar, the identification of causal genes in both species is of great interest in understanding the genetic mechanisms involved in a given developmental process. Of particular interest are the cases in which different numbers of genes are assigned to the same phenotypic groups. In zebrafish, single genetic loci are responsible for the phenotypes of *one-eye-pinhead* (Schier et al., 1996) and *parachute* mutants (Jiang et al., 1996), but in Medaka, mutations in three genes give rise to phenotypes that are analogous to each zebrafish gene (Kitagawa et al., 2004).

Another interest would be to learn how the mutational disruption of orthologous genes results in different phenotypes in the two species. This will reveal how genetic mechanisms in the genesis of an organ can vary, and how the usage and/or regulation of orthologous genes has diversified in phylogeny. Differences in expression patterns and mutant phenotypes of orthologous genes in two related species have been discussed in terms of a model of gene duplication and complementing degenerative mutations (Force et al., 1999).

3.3. Mutations affecting tissue organization

Mutants with abnormalities in tissue organization and integrity fell into three distinct phenotypic groups. The first two groups appear to be unique to Medaka. In the first group of mutants, the initial specification of various brain regions appears to proceed normally, but these regions are gradually dislocated and/or disorganized by later stages of development. This was observed for the *fukuwarai*, *yuzen* and *kagome* mutants (Kitagawa et al., 2004; Watanabe et al., 2004). The second group, represented by *hirame*, is defective in the convergent movements of subsets of cells

toward the dorsal axis. While epiblast cells appear to converge normally in this mutant, cellular convergence in the hypoblast is seriously impaired, resulting in a reduced dorso-ventral thickness of the tissue along the body axis (Watanabe et al., 2004). By contrast, in zebrafish *silberblick* (Heisenberg et al., 2000), *knypek* (Topczewski et al., 2001) and *trilobite* mutants (Jessen et al., 2002), medial convergence of cells in both the epiblast and hypoblast layers is affected. In *spadetail* zebrafish mutants, the convergence of paraxial and intermediate mesoderm fails in the trunk region while epiblast movements are relatively normal. The last group consists of the *oobesshimi*, *samidare* and *shigure* mutants that are characterized by the exfoliation of neural cells in the ventricle (Kitagawa et al., 2004), reminiscent of zebrafish *parachute* mutants (Erdmann et al., 2003; Lele et al., 2002).

3.4. Development of primordial germ cells and the lateral line

The early development of primordial germ cell (PGC) is considerably different between Medaka and zebrafish. In zebrafish, germplasm-derived *vasa* mRNA is localized close to the cleavage plane at the four-cell stage, and this is reflected by four-cell clusters with high *vasa* expression close to the blastoderm margin at the onset of gastrulation (Weidinger et al., 1999). In Medaka, *vasa*-expressing cells appear only at the late-gastrula stage, and are scattered in the posterior one-third of the embryonic shield (Shinomiya et al., 2000). These observations are consistent with the report that fish of the ostariophysan clade (which includes zebrafish) localize *vasa* mRNA to the germplasm, and those of the euteleost clade (which includes Medaka) do not (Knaut et al., 2002). The subsequent migration of PGCs to the gonadal anlage has some similarity between the two species, although the pathways of cellular migration differ (Sasado et al., 2004). Medaka mutations affecting PGC development were screened for altered vasa expression, and mutations in 10 genes that affect PGC migration were identified (Sasado et al., 2004). Among the mutants, those of *kazura* and *yanagi* also have a defect in the distribution of lateral line primordia (Yasuoka et al., 2004).

In zebrafish, chemokine SDF1 and its G-protein-coupled receptor CXCR4b were shown to be required for the proper guidance of the migration of PGCs and lateral line primordia (Doitsidou et al., 2002; David et al., 2002). Indeed, a zebrafish mutant showing aberrant migration of PGCs and the lateral line has been isolated, and was recently found to have a mutation in the *cxcr4b* gene (Knaut et al., 2003).

The phenotypes of *kazura* and *yanagi* mutants with affected migration of PGCs and lateral line primordia resemble those of the zebrafish mutants in which SDF1/CXCR4b interaction is impaired (Yasuoka et al., 2004). While the *kazura* locus is linked to Medaka *cxcr4*, *yanagi* is neither linked to *cxcr4* nor *sdf1*, implying that *yanagi* codes for a new component of the SDF1-CXCR4b signaling pathway. In mice, it was also reported that germ cell migration and survival require SDF1/CXCR4 interaction (Molyneaux et al., 2003), indicating a high degree of evolutionary conservation in the mechanism regulating PGC migration.

vasa Expression was also employed to mark germ cells in developing gonad, and was useful in identifying gonad development mutants (Morinaga et al., 2004). In normal Medaka growth, distribution and differentiation of germ cells are clearly dimorphic reflecting genetically defined sex (Aida, 1921), but some gonad mutants lack this dimorphism, suggesting uncoupling of the gonadogenesis from the process downstream of the sex determination gene DMY (Matsuda et al., 2002; Nanda et al., 2002). Other mutants show abnormal *ftz-f1* expression that marks gonadal somatic cells. These mutants should prove useful in identifying the possible interaction of somatic and germ cells and the mechanisms underlying sexually dimorphic gonad development.

3.5. Prospect: towards elucidating vertebrate genome function

The analysis of mutational defects at the cellular level and the characterization of mutated genes are essential in defining the functions of genes in organogenesis and development. Focusing on neurogenesis, we have carried out cell lineage and migration analyses to map cell fates in Medaka (Hirose et al., 2004). A battery of genomic tools and resources for mutation mapping and gene cloning is already available (Zadeh Khorasani et al., 2004). The relatively small size of the Medaka genome, the availability of inbred strains with a high frequency of polymorphisms in Medaka, and the substantial syntenic preservation of gene alignments between Medaka and Fugu will facilitate positional cloning of mutated genes. The recent success of cloning the *b* gene (Fukamachi et al., 2001), *eyeless* gene (Loosli et al., 2001) and sex determining gene DMY (Matsuda et al., 2002) are just a prelude to forthcoming achievements. Genome sequencing on the basis of Bac contigs (Zadeh Khorasani et al., 2004), and by the whole-genome shotgun approach should accelerate such efforts. The accomplishment of ongoing whole-genome sequencing in Medaka and zebrafish will greatly facilitate comparative functional genomics in both species.

Medaka and zebrafish can be reared and bred in the same aquarium system, and can be studied by similar experimental approaches. Their commonality as small rapidly developing fish, as well as their unique genetic traits make them useful as complementary experimental animals. As described in this article, their use as model vertebrates is obviously advantageous in understanding the genomic functions involved in embryogenesis.

4. Materials and methods

4.1. Fish strains and fish maintenance

The Cab and Heino strains were obtained from the Wittbrodt laboratory and the Kaga strain from the Shima laboratory. The Cab strain, originating from the southern population of Medaka (Loosli et al., 2000), is homozygous for the recessive mutation of b^l of the *B* locus, that results in amelanotic melanophores. The Kaga strain is a wild-type strain originating from the northern population and was used for genetic linkage analysis (Yasuoka et al., 2004). The Heino strain is homozygous for the albino locus and was used for a specific locus test (Shima and Shimada, 1988). To establish a subline suitable for a mutagenesis screen, we have carried out brother–sister mating of the Cab and Kaga strains for more than nine generations. Strains with reasonable fecundity and a very low background of embryonic abnormalities in the temperature range between 18 and 32 °C, (Kyoto-Cab (K-Cab) and Kyoto-Kaga (K-Kaga) were established.

To carry out a large-scale mutagenesis screening, we used a fish cultivating system (Aquatic Habitats) equipped with 120 racks that can hold approximately 6000 tanks. Fish cultivation water was prepared by adding Red Sea salts (0.03%) to reverse osmosis water. Fish water was circulated with 10% daily exchange to new water.

4.2. Mutagenesis and breeding

Fish were mutagenized using available protocols for zebrafish and Medaka with modifications (Solnica-Krezel et al., 1994; Mullins et al., 1994; Loosli et al., 2000). Males of the K-Cab strain were treated with a solution containing 3 mM *N*-ethyl-*N*-nitrosourea (ENU) in 10 mM sodium phosphate (pH 7.0) at 27 °C for 1 h three times at three-day intervals. Starting from four weeks after the last ENU treatment, mutagenized males (G0) were crossed with K-Cab females to generate an F1 progeny (Fig. 1). Ten G0 males were crossed with homozygous Heino albino females for a specific locus test. The test was performed after many F1 fish were produced by crossing the G0 males with wild type females, and a large fraction of mutagenized males died before the test was completed. Thus, not all mutagenized males were subjected to the specific locus test. The mutational frequencies of hitting the albino locus under the described conditions were in the range of 1/196–1/726 among groups of 10 males tested. A total of 1300 F2 families were raised and used for mutant screening.

4.3. Mutant screening

4.3.1. Egg collection and phenotype recording

Matings of six to seven sibling pairs were made for each F2 family, and clutches of 15–40 eggs were collected per day from a pair. Ten clutches of eggs obtained from a pair were grown at three different temperatures (18, 28 and 33 °C) and screened for developmental abnormalities. A dissection stereomicroscope (Leica, MZ12.5) was used for embryo inspection. Observed phenotypes were recorded by a digital camera (Fuji Film, HC-300 Z) at the site of screening, and digitally archived into a database (Henrich et al., 2004).

4.3.2. Screening using live embryos

Live embryos were morphologically inspected at the three developmental stages, st. 19–21 (27–34 hpf), st. 25–27 (50–58 hpf) and st. 32–35 (4 dpf). Fig. 2 shows normal embryos at stages chosen for mutant screening. Liver-associated lipid metabolism was assessed by the accumulation of fluorescent PED6 metabolite in the liver and gall bladder at st. 34 (Watanabe et al., 2004). The metabolism of hemoglobin into bilirubin was monitored by the color of bile in the gall bladder in live embryos at st. 34. Sensitivity to γ-ray was assessed in terms of recovery at st. 32 from irradiation at 9.1 Gy (gray, which is defined as absorption of 1 J/kg. The absorbed-dose rate was monitored by a radio-photoluminescent glass dosimeter and a Fricke dosimeter) at st. 24 (Aizawa et al., 2004).

4.3.3. Whole-mount staining of fixed embryos

In situ hybridization and immunostaining were carried out for detecting specific molecular markers. Eggs were dechorionated by incubation in a pronase solution at 5 mg/ml (Sigma) and a crude hatching enzyme preparation (an extract of embryos at the hatching period, Ishida, 1944) for 1 h each at 28 °C, fixed with 4% paraformaldehyde (PFA) at stages indicated. PGCs and germ cells were visualized by the hybridization of fixed embryos/larvae with the Medaka *vasa* probe (Shinomiya et al., 2000) at st. 29 and 15 dpf, respectively (Sasado et al., 2004; Morinaga et al., 2004). Thymocytes in the thymus were detected by in situ hybridization using Medaka *rag1* probe at st. 32 (Iwanami et al., 2004). Axons and cell bodies of cranial nerves were immunostained using the mixture of anti-acetylated tubulin and HNK-1 antibodies at st. 32 (Kitagawa et al., 2004). RGC axons projecting to the tectum were visualized by injecting lipophilic fluorescent dyes DiI and DiO into the diagonal positions of the retina of fixed embryos at 9 dpf (Baier et al., 1996; Yoda et al., 2004).

4.4. Recovery of mutations and complementation test

After screening, carrier F2 fish were crossed with K-Cab fish to generate an F3 generation family. Carrier F2 males were then sacrificed under anesthesia to collect sperms for frozen stocks. Mutations were recovered in the F3 generation by random mating within F3 families and the identified pairs were crossed with the Kaga strain to generate an F4 generation to be used in linkage analysis. Complementation tests were performed by crossing heterozygous carriers of different mutations that cause similar phenotypes.

Acknowledgements

We would like to thank Drs Robert Kelsh, Francisco Pelegri, Fredericus van Eeden and John Postlethwait for critical reading and comments on this manuscript. We also thank Dr Koji Okamoto for his scientific administration, Haruka Momose and Takahiro Negishi for carrying out complementation tests. This work was supported initially by the PRESTO grant from Japan Science and Technology Agency (JST) to M.F.-S. and by the ERATO grant from JST to H.K.

References

Aida, T., 1921. On the inheritance of color in a fresh-water fish, *Aplocheilus latipes* Temminck and Schlegel, with special reference to sex-linked inheritance. Genetics 6, 554–573.

Aizawa, K., Mitani, H., Kogure, N., Shimada, A., Hirose, Y., Sasado, T., et al., 2004. Identification of radiation-sensitive mutants in the Medaka, *Oryzias latipes*. Mech. Dev. 121, 895–902.

Amores, A., Force, A., Yan, Y.L., Joly, L., Amemiya, C., Fritz, A., et al., 1998. Zebrafish hox clusters and vertebrate genome evolution. Science 282, 1711–1714.

Baier, H., Klostermann, S., Trowe, T., Karlstrom, R.O., Nusslein-Volhard, C., Bonhoeffer, F., 1996. Genetic dissection of the retinotectal projection. Development 123, 415–425.

Bennett, A.R., Farley, A., Blair, N.F., Gordon, J., Sharp, L., Blackburn, C.C., 2002. Identification and characterization of thymic epithelial progenitor cells. Immunity 16, 803–814.

Brand, M., Heisenberg, C.P., Warga, R.M., Pelegri, F., Karlstrom, R.O., Beuchle, D., et al., 1996. Mutations affecting development of the midline and general body shape during zebrafish embryogenesis. Development 123, 129–142.

Brenner, S., 1974. The genetics of *Caenorhabditis elegans*. Genetics 77, 71–94.

David, N.B., Sapede, D., Saint-Etienne, L., Thisse, C., Thisse, B., Dambly-Chaudiere, C., et al., 2002. Molecular basis of cell migration in the fish lateral line: role of the chemokine receptor CXCR4 and of its ligand, SDF1. Proc. Natl Acad. Sci. USA 99, 16297–16302.

Doitsidou, M., Reichman-Fried, M., Stebler, J., Koprunner, M., Dorries, J., Meyer, D., et al., 2002. Guidance of primordial germ cell migration by the chemokine SDF-1. Cell 111, 647–659.

Driever, W., Solnica-Krezel, L., Schier, A.F., Neuhauss, S.C., Malicki, J., Stemple, D.L., et al., 1996. A genetic screen for mutations affecting embryogenesis in zebrafish. Development 123, 37–46.

van Eeden, F.J., Granato, M., Schach, U., Brand, M., Furutani-Seiki, M., Haffter, P., et al., 1996. Mutations affecting somite formation and patterning in the zebrafish, *Danio rerio*. Development 123, 153–164.

Elmasri, H., Winkler, C., Liedtke, D., Sasado, T., Morinaga, C., Suwa, H., et al., 2004. Mutations affecting somite formation in the Medaka (*Oryzias latipes*). Mech. Dev. 121, 659–671.

Erdmann, B., Kirsch, F.P., Rathjen, F.G., More, M.I., 2003. N-cadherin is essential for retinal lamination in the zebrafish. Dev. Dyn. 226, 570–577.

Farber, S.A., Pack, M., Ho, S.Y., Johnson, I.D., Wagner, D.S., Dosch, R., et al., 2001. Genetic analysis of digestive physiology using fluorescent phospholipid reporters. Science 292, 1385–1388.

Force, A., Lynch, M., Pickett, F.B., Amores, A., Yan, Y.L., Postlethwait, J., 1999. Preservation of duplicate genes by complementary, degenerative mutations. Genetics 151, 1531–1545.

Fukamachi, S., Shimada, A., Shima, A., 2001. Mutations in the gene encoding B, a novel transporter protein, reduce melanin content in medaka. Nat. Genet. 28, 381–385.

Furutani-Seiki, M., Jiang, Y.J., Brand, M., Heisenberg, C.P., Houart, C., Beuchle, D., et al., 1996. Neural degeneration mutants in the zebrafish, *Danio rerio*. Development 123, 229–239.

Gill, J., Malin, M., Hollander, G.A., Boyd, R., 2002. Generation of a complete thymic microenvironment by MTS24(+) thymic epithelial cells. Nat. Immunol. 3, 635–642.

Haffter, P., Granato, M., Brand, M., Mullins, M.C., Hammerschmidt, M., Kane, D.A., et al., 1996. The identification of genes with unique and essential functions in the development of the zebrafish, *Danio rerio*. Development 123, 1–36.

Heisenberg, C.P., Brand, M., Jiang, Y.J., Warga, R.M., Beuchle, D., van Eeden, F.J., et al., 1996. Genes involved in forebrain development in the zebrafish, *Danio rerio*. Development 123, 191–203.

Heisenberg, C.P., Tada, M., Rauch, G.J., Saude, L., Concha, M.L., Geisler, R., et al., 2000. Silberblick/Wnt11 mediates convergent extension movements during zebrafish gastrulation. Nature 405, 76–81.

Henrich, T., Ramialison, M., Segerdell, E., Westerfield, M., Furutani-Seiki, M., Wittbrodt, J., Kondoh, H., 2004. GSD: a genetic screen database. Mech. Dev. 121, 959–963.

Hirose, Y., Varga, Z.M., Kondoh, H., Furutani-Seiki, M., 2004. Single cell lineage and regionalization of cell populations during Medaka neurulation. Development, in press.

Hrabe de Angelis, M.H., Flaswinkel, H., Fuchs, H., Rathkolb, B., Soewarto, D., Marschall, S., et al., 2000. Genome-wide, large-scale production of mutant mice by ENU mutagenesis. Nat. Genet. 25, 444–447.

Hyodo-Taguchi, Y., 1983. Effects of UV irradiation on embryonic development of different inbred strains of the fish *Oryzias latipes*. J. Radiat. Res. (Tokyo) 24, 221–228.

Ishida, J., 1944. Hatching enzyme in the fresh-water teleost, *Oryzias latipes*. Annot. Zool. Japon. 22, 137–154.

Ishikawa, Y., 2000. Medakafish as a model system for vertebrate developmental genetics. Bioessays 22, 487–495.

Iwanami, N., Takahama, Y., Kunimatsu, S., Li, J., Takei, R., Ishikura, Y., et al., 2004. Mutations affecting thymus organogenesis in Medaka, *Oryzias latipes*. Mech. Dev. 121, 779–789.

Jessen, J.R., Topczewski, J., Bingham, S., Sepich, D.S., Marlow, F., Chandrasekhar, A., Solnica-Krezel, L., 2002. Zebrafish trilobite identifies new roles for Strabismus in gastrulation and neuronal movements. Nat. Cell Biol. 4, 610–615.

Jiang, Y.J., Brand, M., Heisenberg, C.P., Beuchle, D., Furutani-Seiki, M., Kelsh, R.N., et al., 1996. Mutations affecting neurogenesis and brain morphology in the zebrafish, *Danio rerio*. Development 123, 205–216.

Karlstrom, R.O., Trowe, T., Klostermann, S., Baier, H., Brand, M., Crawford, A.D., et al., 1996. Zebrafish mutations affecting retinotectal axon pathfinding. Development 123, 427–438.

Kimmel, C.B., 1989. Genetics and early development of zebrafish. Trends Genet. 5, 283–288.

Kitagawa, D., Watanabe, T., Saito, K., Asaka, S., Sasado, T., Morinaga, C., et al., 2004. Genetic dissection of the formation of the forebrain in Medaka, *Oryzias latipes*. Mech. Dev. 121, 673–685.

Knaut, H., Steinbeisser, H., Schwarz, H., Nusslein-Volhard, C., 2002. An evolutionary conserved region in the vasa 3'UTR targets RNA translation to the germ cells in the zebrafish. Curr. Biol. 12, 454–466.

Knaut, H., Werz, C., Geisler, R., Nusslein-Volhard, C., 2003. A zebrafish homologue of the chemokine receptor Cxcr4 is a germ-cell guidance receptor. Nature 421, 279–282.

Jenkinson, W.E., Jenkinson, E.J., Anderson, G., 2003. Differential requirement for mesenchyme in the proliferation and maturation of thymic epithelial progenitors. J. Exp. Med. 198, 325–332.

Lele, Z., Folchert, A., Concha, M., Rauch, G.J., Geisler, R., Rosa, F., et al., 2002. Parachute/n-cadherin is required for morphogenesis and maintained integrity of the zebrafish neural tube. Development 129, 3281–3294.

Loosli, F., Koster, R.W., Carl, M., Kuhnlein, R., Henrich, T., Mucke, M., et al., 2000. A genetic screen for mutations affecting embryonic development in medaka fish (*Oryzias latipes*). Mech. Dev. 97, 133–139.

Loosli, F., Del Bene, F., Quiring, R., Rembold, M., Martinez-Morales, J.-R., Carl, M., et al., 2004. Mutations affecting retina development in Medaka. Mech. Dev. 121, 703–714.

Manley, N.R., 2000. Thymus organogenesis and molecular mechanisms of thymic epithelial cell differentiation. Semin. Immunol. 12, 421–428.

Matsuda, M., Nagahama, Y., Shinomiya, A., Sato, T., Matsuda, C., Kobayashi, T., et al., 2002. DMY is a Y-specific DM-domain gene required for male development in the medaka fish. Nature 417, 559–563.

Mayer, U., Ruiz, R.A.T., Berleth, T., Misera, S., Jürgens, G., 1991. Mutations affecting body organization in the *Arabidopsis* embryo. Nature 353, 402–407.

Molyneaux, K.A., Zinszner, H., Kunwar, P.S., Schaible, K., Stebler, J., Sunshine, M.J., et al., 2003. The chemokine SDF1/CXCL12 and its receptor CXCR4 regulate mouse germ cell migration and survival. Development 130, 4279–4286.

Morinaga, C., Tomonaga, T., Sasado, T., Suwa, H., Niwa, K., Yasuoka, A., et al., 2004. Mutations affecting gonadal development in Medaka, *Oryzias latipes*. Mech. Dev. 121, 829–839.

Mullins, M.C., Hammerschmidt, M., Haffter, P., Nusslein-Volhard, C., 1994. Large-scale mutagenesis in the zebrafish: in search of genes controlling development in a vertebrate. Curr. Biol. 4, 189–202.

Nanda, I., Kondo, M., Hornung, U., Asakawa, S., Winkler, C., Shimizu, A., et al., 2002. A duplicated copy of DMRT1 in the sex-determining region of the Y chromosome of the medaka, *Oryzias latipes*. Proc. Natl Acad. Sci. USA 99, 11778–11783.

Naruse, K., Fukamachi, S., Mitani, H., Kondo, M., Matsuoka, T., Kondo, S., et al., 2000. A detailed linkage map of medaka, *Oryzias latipes*: comparative genomics and genome evolution. Genetics 154, 1773–1784.

Nolan, P.M., Peters, J., Strivens, M., Rogers, D., Hagan, J., Spurr, N., et al., 2000. A systematic, genome-wide, phenotype-driven mutagenesis programme for gene function studies in the mouse. Nat. Genet. 25, 440–443.

Nüsslein-Volhard, C., Wieschaus, E., 1980. Mutations affecting segment number and polarity in *Drosophila*. Nature 287, 795–801.

Ohno, S., 1970. Evolution by Gene Duplication, Springer, Heidelberg.

Russell, L.B., Montgomery, C.S., 1982. Supermutagenicity of ethylnitrosourea in the mouse spot test: comparisons with methylnitrosourea and ethylnitrosourethane. Mutat. Res. 92, 193–204.

Sasado, T., Morinaga, C., Niwa, K., Shinomiya, A., Yasuoka, A., Suwa, H., et al., 2004. Mutations affecting early distribution of primordial germ cells in Medaka (*Oryzias latipes*) embryo. Mech. Dev. 121, 817–828.

Schier, A.F., Neuhauss, S.C., Harvey, M., Malicki, J., Solnica, K.L., Stainier, D.Y., et al., 1996. Mutations affecting the development of the embryonic zebrafish brain. Development 123, 165–178.

Shima, A., Shimada, A., 1988. Induction of mutations in males of the fish *Oryzias latipes* at a specific locus after gamma-irradiation. Mutat. Res. 198, 93–98.

Shinomiya, A., Tanaka, M., Kobayashi, T., Nagahama, Y., Hamaguchi, S., 2000. The vasa-like gene, olvas, identifies the migration path of primordial germ cells during embryonic body formation stage in the medaka, *Oryzias latipes*. Dev. Growth Differ. 42, 317–326.

Solnica-Krezel, L., Schier, A.F., Driever, W., 1994. Efficient recovery of ENU-induced mutations from the zebrafish germline. Genetics 136, 1401–1420.

Topczewski, J., Sepich, D.S., Myers, D.C., Walker, C., Amores, A., Lele, Z., et al., 2001. The zebrafish glypican knypek controls cell polarity during gastrulation movements of convergent extension. Dev. Cell 1, 251–264.

Watanabe, T., Asaka, S., Kitagawa, D., Saito, K., Kurashige, R., Sasado, T., et al., 2004. Mutations affecting liver development and function in Medaka, *Oryzias latipes*, screened by multiple criteria. Mech. Dev. 121, 791–802.

Weidinger, G., Wolke, U., Koprunner, M., Klinger, M., Raz, E., 1999. Identification of tissues and patterning events required for distinct steps in early migration of zebrafish primordial germ cells. Development 126, 5295–5307.

Wittbrodt, J., Shima, A., Schartl, M., 2002. Medaka: a model organism from the far East. Nat. Rev. Genet. 3, 53–64.

Yamamoto, T.O., 1965. Estriol-induced XY females of the medaka (*Oryzias latipes*) and their progenies. Gen. Comp. Endocrinol. 5, 527–533.

Yasuoka, A., Hirose, Y., Yoda, H., Aihara, Y., Suwa, H., Niwa, K., et al., 2004. Mutations affecting the formation of posterior lateral line system in Medaka, *Oryzias latipes*. Mech. Dev. 121, 729–738.

Yoda, H., Hirose, Y., Yasuoka, A., Sasado, T., Morinaga, C., Deguchi, T., et al., 2004. Mutations affecting retinotectal axonal pathfinding in Medaka, *Oryzias latipes*. Mech. Dev. 121, 715–728.

Zadeh Khorasani, M., Hennig, S., Imre, G., Asakawa, S., Palczewski, S., Berger, A., et al., 2004. A first generation physical map of the medaka genome in BACs essential for positional cloning and clone-by-clone based genomic sequencing. Mech. Dev. 121, 903–913.

ELSEVIER

Mechanisms of Development 121 (2004) 673–685

www.elsevier.com/locate/modo

Research paper

Genetic dissection of the formation of the forebrain in Medaka, *Oryzias latipes*

Daiju Kitagawa[a], Tomomi Watanabe[a], Kota Saito[a], Satoshi Asaka[a], Takao Sasado[b], Chikako Morinaga[b], Hiroshi Suwa[b], Katsutoshi Niwa[b], Akihito Yasuoka[c], Tomonori Deguchi[d], Hiroki Yoda[d], Yukihiro Hirose[e], Thorsten Henrich[b], Norimasa Iwanami[f], Sanae Kunimatsu[f], Masakazu Osakada[g], Chritoph Winkler[h], Harun Elmasri[h], Joachim Wittbrodt[i], Felix Loosli[i], Rebecca Quiring[i], Matthias Carl[i], Clemens Grabher[i], Sylke Winkler[i], Filippo Del Bene[i], Akihiro Momoi[d], Toshiaki Katada[a], Hiroshi Nishina[a], Hisato Kondoh[b,d], Makoto Furutani-Seiki[b,*]

[a]*Department of Physiological Chemistry, Graduate School of Pharmaceutical Sciences, The University of Tokyo, Tokyo 113-0033, Japan*
[b]*Japan Science and Technology Agency, ERATO, Kondoh Differentiation Signaling Project, Kawaracho14, Yoshida, Sakyoku, Kyoto 606-8305, Japan*
[c]*Graduate School of Agricultural and Life Sciences, The University of Tokyo, Tokyo 113-0033, Japan*
[d]*Graduate School of Frontier Biosciences, Osaka University, Osaka, 565-0871, Japan*
[e]*Graduate School of Biostudies, Kyoto University, Kyoto 606-8502, Japan*
[f]*Division of Experimental Immunology, Institute for Genome Research, The University of Tokushima, Tokushima 770-8503, Japan*
[g]*Department of Molecular Medicine and Pathophysiology, Research Institute, Osaka Medical Center for Cancer and Cardiovascular Diseases, Osaka 537-8511, Japan*
[h]*Department of Physiological Chemistry I, Biocenter, University of Wuerzburg, Wuerzburg, Germany*
[i]*Developmental Biology Programme, EMBL, D-69117, Heidelberg, Germany*

Received 1 February 2004; received in revised form 16 March 2004; accepted 18 March 2004

Abstract

The forebrain, consisting of the telencephalon and diencephalon, is essential for processing sensory information. To genetically dissect formation of the forebrain in vertebrates, we carried out a systematic screen for mutations affecting morphogenesis of the forebrain in Medaka. Thirty-three mutations defining 25 genes affecting the morphological development of the forebrain were grouped into two classes. Class 1 mutants commonly showing a decrease in forebrain size, were further divided into subclasses 1A to 1D. Class 1A mutation (1 gene) caused an early defect evidenced by the lack of *bf1* expression, Class 1B mutations (6 genes) patterning defects revealed by the aberrant expression of regional marker genes, Class 1C mutation (1 gene) a defect in a later stage, and Class 1D (3 genes) a midline defect analogous to the zebrafish *one-eyed pinhead* mutation. Class 2 mutations caused morphological abnormalities in the forebrain without considerably affecting its size, Class 2A mutations (6 genes) caused abnormalities in the development of the ventricle, Class 2B mutations (2 genes) severely affected the anterior commissure, and Class 2C (6 genes) mutations resulted in a unique forebrain morphology. Many of these mutants showed the compromised *sonic hedgehog* expression in the zona-limitans-intrathalamica (zli), arguing for the importance of this structure as a secondary signaling center. These mutants should provide important clues to the elucidation of the molecular mechanisms underlying forebrain development, and shed new light on phylogenically conserved and divergent functions in the developmental process.

Keywords: Forebrain; Telencephalon; Diencephalon; Mutants; Medaka; Mutagenesis screen

1. Introduction

The vertebrate forebrain, consisting of the telencephalon and diencephalon, is formed at the most rostral portion of the developing central nervous system (CNS). The telencephalon is the highest-order processor of neural functions,

* Corresponding author. Tel./fax: +81-75-771-9362.
E-mail address: furutaniseiki@msi.biglobe.ne.jp (M. Furutani-Seiki).

0925-4773/$ - see front matter © 2004 Elsevier Ireland Ltd. All rights reserved.
doi:10.1016/j.mod.2004.03.010

and the diencephalon is the conduit for ascending sensory information. Each territory of the forebrain is further regionalized along the respective anteroposterior (AP) and dorsoventral (DV) axes. These structures in the forebrain and their connections are essential for processing sensory information, integrating of new sensory information with established memories, and then formulating and effecting behavioral responses (Wilson and Rubenstein, 2000; Rallu et al., 2002).

The vertebrate forebrain was proposed to be subdivided in a segment-like manner into transverse neuromeric domains (prosomeres) analogous to rhombomeres in the hindbrain; on the basis of restricted expression patterns of transcription factors (neuromeric model, Bulfone et al., 1993; Figdor and Stern, 1993; Puelles and Rubenstein, 1993; Hauptmann and Gerster, 2000).

In all vertebrates, the developing telencephalon is subdivided into the dorsal (pallial region, expressing *emx1*) and ventral (subpallial region, expressing *dlx2*) domains. In the mammalian telencephalon, dorsal, pallial regions give rise to the cortex, while ventral, subpallial regions give rise to the basal ganglia. Similar pallial and subpallial subdivisions of the telencephalon exist in all vertebrates (Fernandez et al., 1998; Puelles et al., 2000), although the adult derivatives of these subdivisions vary among species.

The diencephalon is proposed to be divided into four longitudinal neuronal zones—dorsally, epithalamus, dorsal thalamus, ventral thalamus; and ventrally, hypothalamus (Figdor and Stern, 1993; Hauptmann et al., 2002). The dorsal and ventral thalami are divided by the zona limitans intrathalamica (zli). Although it is yet to be proven, the zli has been suggested to be a secondary signaling center, since the secreted signaling protein *sonic hedgehog* (*shh*) is expressed in the zli.

Theories of the formation of the subdivisions of the forebrain, however, are established on the bases of restricted expression patterns, mostly of transcription factors. Most of these transcription factors were cloned either by the homology of genes identified in the forward genetic mutant screening of invertebrates, such as *Drosophila melanogaster* and *Caenorhabditis elegans*, or by expression pattern screening. Functional studies of these genes have been carried out by the reverse genetic approach in the mouse or gain-of-function studies in chick, *Xenopus* and zebrafish. These studies, however, were still limited to the genes initially cloned by homology or expression patterns, but not their functions.

Genome-wide forward genetic screening based on the functions of genes, carried out using zebrafish for the first time in vertebrates, together with gene knock-out mice, established a genetic basis for the three key signaling pathways for the patterning of the forebrain. The Nodal pathway acts upstream of Shh signaling to specify the ventral telencephalon (Rohr et al., 2001; Varga et al., 2001), but Nodal and Shh signaling have distinct and cooperative roles in the development of the ventral diencephalon (Mathieu et al., 2002). However, the precise roles of Shh signaling, such as the source and time of action for the patterning the forebrain, remain to be elucidated. Wnt signaling is also reported to be important for patterning of the forebrain along the anteroposterior (A–P) axis (Kim et al., 2000; Heisenberg et al., 2001). The first row of cells at the rostral margin of the neural plate were shown to pattern the anterior forebrain anteroposteriorly (Houart et al., 1998) and its function has been ascribed to the secretion of the Wnt antagonist, *tlc* (Houart et al., 2002), corroborating the importance of Wnt signaling for A–P patterning in the forebrain in zebrafish. Nevertheless, insights obtained from existing mutants are still fragmentary due to the limited number of mutants.

In vertebrates in which the functions of multiple genes often overlap, mutagenesis screens in a single species is not sufficient for uncovering all functioning genes in a genetic cascade or in the development of an organ, but this limitation should be largely alleviated by the use of another related animal species. Thus, to define the genetic components of the signaling required for patterning of the forebrain and their interplay, we have undertaken a large-scale mutagenesis screen in Medaka. Here, we report the initial characterization of 33 mutations in 25 complementation groups exhibiting specific defects in the development of the forebrain. These mutants show a reduction in the size of the telencephalon, and defects in the formation of the ventricle or axogenesis. These mutants are often phenotypically distinct from those of mutants isolated in zebrafish (Brand et al., 1996a,b; Furutani-Seiki et al., 1996; Heisenberg et al., 1996; Schier et al., 1996), supporting the importance of this fish species which complements zebrafish.

2. Results

2.1. Development and regionalization of forebrain in wild-type Medaka embryos

The forebrain formed at the most rostral portion of the neural plate is composed of the telencephalon and diencephalon, occupying its dorsoanterior and ventroposterior portions, respectively. In Medaka, the forebrain becomes distinguishable from the midbrain at the histological level at stage 19 (st. 19), 27 hours post fertilization (hpf) at 28 °C (Fig. 1A), (Iwamatsu, 1994), and morphologically at st. 21 (Fig. 1B). During st. 19 and 21, the tissue initially located at the rostral end of the brain tissue is displaced to the ventral side of the brain. At st. 23 (41 hpf), the forebrain ventricle starts to form (Fig. 1C). During st. 23 and st. 27, the initially linear anteroposterior (A–P) axis through the brain is bent in the diencephalon area forming the ventral diencephalon (hypothalamus) overlain by both the dorsal diencephalon and mesensephalon, thereby

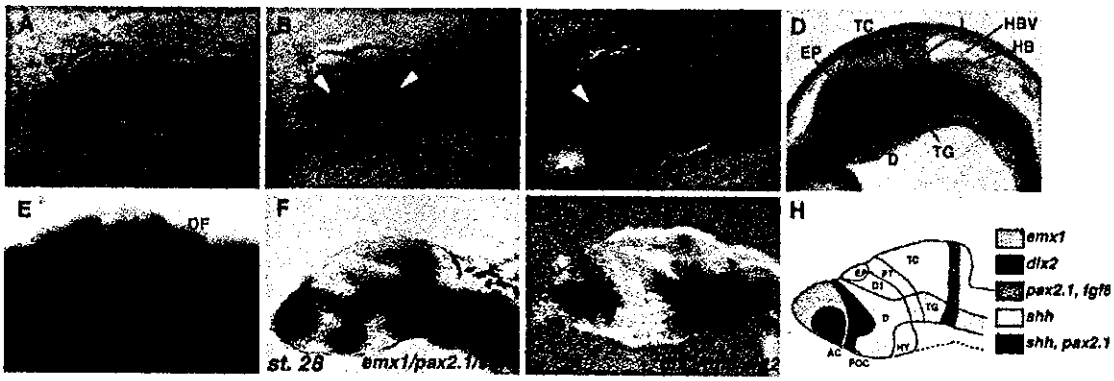

Fig. 1. Development and regionalization of the forebrain in wild-type Medaka embryos. (A–D) Morphology of the brain in Medaka live embryos. Dorsal view of wild-type embryo at (A) st. 19, (B) st. 21, (C) st. 23, (D) lateral view of the embryo at st. 27. (E) Major axonal scaffolds in the forebrain. Whole-mount immunostaining with anti-acetylated-tubulin and anti-HNK antibodies at st. 31. Ventral view of anterior portion of the head. (F,G) Whole-mount in situ hybridization analysis at st. 28. (F) *emx1*, *pax2.1*, *shh*; and (G) *dlx2*, *fgf8*, *slit2* as probes. (H) Schematic representation of gene expression patterns in subdivisions of the forebrain and midbrain. AC, anterior commissure; D, diencephalon; DT, dorsal thalamus; EP, epiphysis; F, forebrain; FV, forebrain ventricle; HB, hindbrain; HBV, hindbrain ventricle; HY, hypothalamus; I, isthmus; M, midbrain; OF, olfactory nerve; ON, optic nerve; POC, post-optic commissure; PT, pretectum; SOT, supraoptic tract; T, telencephalon; TC, tectum; TG, tegmentum; VT, ventral thalamus.

establishing the dorsoventral axis of the diencephalon (Fig. 1D). The cell layer of the roof of the telencephalon loses their thickness, and the telencephalon assumes its characteristic morphology. During st. 28–34 (64–131 hpf), cells proliferate extensively in the ventricular zone, and the ventricle loses its space (Ishikawa and Hyodo-Taguchi, 1994). The major axonal scaffolds in the forebrain, including commissural neurons, the supraoptic tract and sensory nerves, are formed by st. 34 (Fig. 1E).

In zebrafish, it was demonstrated that the expression patterns of marker genes define the transverse and longitudinal subdivisions within the forebrain and midbrain (Macdonald et al., 1994; Hauptmann and Gerster, 2000). Expression patterns of these markers seem to be well conserved in Medaka (Fig. 1F–H). For the initial characterization of Medaka forebrain mutants, we carried out whole-mount in situ hybridization analysis using a mixture of probes, *emx1/pax2.1/shh* and *dlx2/fgf8/slit2*. The dorsal and ventral telencephalon express *emx1* and *dlx2*, respectively. The diencephalon is divided into four domains; dorsal and ventral thalami, pretectum and hypothalamus. The zona limitans intrathalamica (zli), which expresses *shh*, divides the dorsal and ventral thalami. The ventral thalamus is marked by *dlx2* expression.

2.2. *Identification of forebrain mutants in Medaka*

Since a specific patterning defect often causes later occurrence of localized cell degeneration (Furutani-Seiki et al., 1996), we paid special attention to morphological abnormalities accompanied by cell degeneration. In the large-scale mutagenesis screen for embryonic pattern formation, we identified 33 mutations affecting forebrain development in Medaka mutants, exhibiting a variety of morphological defects and/or abnormal axonal pathways. These mutations were assigned to 25 complementation groups (Table 1). We classified these mutations into two groups, on the basis of the type of defects in the telencephalon. Class 1 mutations were those primarily affecting the size of the telencephalon, while Class 2 mutations were those mainly causing abnormalities in the forebrain shape without significantly affecting the size of the telencephalon. All the isolated mutations were zygotic recessive, and in this paper homozygous embryos are referred to as mutants. Two mutations turned out to be temperature sensitive; *kar*$^{j50\text{-}4A}$, which is sensitive to a low temperature (18 °C); and *ika*$^{j94\text{-}8A}$, which is sensitive to a high temperature (33 °C).

2.3. *Class 1 mutations affecting telencephalon size*

We have identified 15 mutations in 11 genes of this class causing reduction in telencephalon size (Fig. 2, arrowheads in A–F). According to the onset of the phenotype, we classified the Class 1 mutations into four subclasses, as summarized in Table 1.

2.3.1. *Class 1A and 1B mutations affecting subregions of the telencephalon*

In *kentoku* (*ket*$^{j23\text{-}3B}$) and *aonibi* (*aon*$^{j9\text{-}2F}$) mutant embryos, morphological defects appeared to be restricted to the telencephalon (Fig. 2B,C), whereas in *kobesshimi* (*kob*$^{j35\text{-}6D}$) and *bouzu* (*bou*$^{jr118\text{-}2A}$) mutant embryos, size reduction occurred also in the midbrain (Fig. 2D,E). On the other hand, *nopperabo* (*nop*$^{j80\text{-}19B}$) mutant embryos exhibited a characteristic phenotype, that is a reduction in forebrain size accompanied by the enlargement of the midbrain, reminiscent of that of *masterblind* (*mbl*) and *headless* (*hdl*) mutants in zebrafish (Fig. 2F).

Class 1 mutant embryos at st. 31 were immunochemically stained with anti-acetylated-tubulin and HNK1

Table 1
Mutations affecting formation of the forebrain

Gene	Symbol	Alleles	Forebrain phenotype	Other phenotypes
Class 1: mutations affecting the size of the telencephalon				
Class 1A: mutations affecting early specification of the telencephalon				
kentoku	*ket*	*j23-3B*	Telencephalon size reduced	
Class 1B: mutations affecting regionalization of the telencephalon				
aonibi	*aon*	*j9-2F, j60-3A*	Telencephalon size reduced	Lipid metabolism affected
kobesshimi	*kob*	*j9-10A, j35-6D, j54-3A*	Telencephalon size reduced	Midbrain slightly reduced
bouzu	*bou*	*jr118-2A*	Telencephalon size reduced	Midbrain anteroposteriorly reduced
nopperabo	*nop*	*j80-19B*	Telencephalon size reduced	Eyes missing, midbrain expanded
kumasaka	*kum*	*j54-20A*	Telencephalon size reduced	
usobuki	*uso*	*j14-26A*	Telencephalon size reduced	
Class 1C: a mutation affecting maintenance of the telencephalon				
hannya	*han*	*j41-3B*	Late telencephalon defect	–
Class 1D: mutations affecting formation of the midline neural tissue				
akatsuki	*aku*	*j22-15A, jf121-1A*	Telencephalon size reduced	Similar to zebrafish *oep*
akebono	*ake*	*j54-7A*	Telencephalon size reduced	Similar to zebrafish *oep*
mochizuki	*moc*	*j96-11B*	Telencephalon size reduced	Similar to zebrafish *oep*
Class 2: mutations affecting morphology of the telencephalon				
Class 2A: mutations affecting formation of the forebrain ventricle				
sarudahiko	*sar*	*j106-4A*	Forebrain ventricle reduced	Circulation, midline defect, tectum reduced
tengu	*ten*	*j2-11A, jr10-4D, j53-4C*	Forebrain ventricle reduced	Circulation, midline defect, tectum reduced
karuna	*kar*	*j50-4A*	Forebrain ventricle enlarged	Temperature sensitive at 18 °C
oobesshimi	*oob*	*j103-11A, j58-1A*	Forebrain ventricle enlarged	Tegmentum and hindbrain bumpy
samidare	*sam*	*j20-26A*	Forebrain ventricle enlarged	Similar to zebrafish *parachute* mutant
shigure	*sgu*	*j55-8A*	Forebrain ventricle enlarged	Similar to zebrafish *parachute* mutant
Class 2B: mutations affecting the formation of the anterior commissure				
ikazuchi	*ika*	*j94-8A*	Ectopic anterior commissure	Temperature sensitive at 33 °C, hindbrain bumpy
shikami	*shi*	*j92-3A*	Anterior commissure not formed	–
Class 2C: mutations causing forebrain dysmorphology				
baltan	*bal*	*j102-2A*	Forebrain dysmorphology, edema	Eyes small, tectum reduced, circulation defect, somite irregular
fukuwarai	*fuk*	*j8-33A, j93-4A*	Forebrain dysmorphology	Regions of CNS misplaced
yuzen	*yuz*	*j107-2D*	Forebrain dysmorphology	Regions of CNS misplaced
kagome	*kag*	*jr114-2D*	Forebrain dysmorphology	Regions of CNS misplaced
hirame	*hir*	*j54-20C*	Flattened, differentiation defect	CNS flat, heart beating next to ears
tobi	*tob*	*jr116-4A*	Protruding telencephalon	Eyes small

antibody to examine the paths and fasciculation of axons (Fig. 2G–L). In the wild type embryos, the olfactory nerve, anterior commissure, supraoptic tract and optic nerve were clearly stained (Fig. 2G). All Class 1 mutants showed interesting abnormalities in these nerves. In *ket* mutant embryos, anterior commissure nerves were not fully fasciculated (black arrowhead in Fig. 2H), displaced and lacked association with the olfactory nerve (white arrowheads in Fig. 2H), and the supraoptic tract was not clearly detected. In *aon* mutant embryos, the olfactory nerve and supraoptic tract were not detected, the anterior commissure lacked fasciculation (white arrowhead in Fig. 2I), and bundle formation of the optic nerve was also affected (black arrowhead in Fig. 2I). *kob* mutants were unique in that only olfactory nerve was affected and lacked fasciculation (arrowhead in Fig. 2J). In *bou* mutant embryos, the axons in the anterior commisure were totally defasciculated, and the commissure did not form (arrowhead in Fig. 2K). In the *nop* mutant embryos, all axonal paths were so severely affected and in astray that the nerves in the forebrain were not morphologically distinguishable each other (arrowhead in Fig. 2L). In addition, the olfactory bulbs appeared to be missing in *nop* mutant embryos (Fig. 2L). Thus, Class 1 mutants share the commonality of a reduced telencephalon size, but alterations of the nerves and their paths were affected distinctly.

Class 1 mutants were also examined for the regional markers of the forebrain by in situ hybridization with two sets of probes, *emx1/pax2.1/shh* and *dlx2/fgf8/slit2* (Fig. 2M–X). Consistent with a smaller telencephalon, Class 1 mutant embryos generally showed a reduction in *emx1* or *dlx2* expression in the telencephalon.

In *ket* and *nop* mutant embryos, the *emx1* expression was strongly reduced (black arrowhead in Fig. 2N,R) and

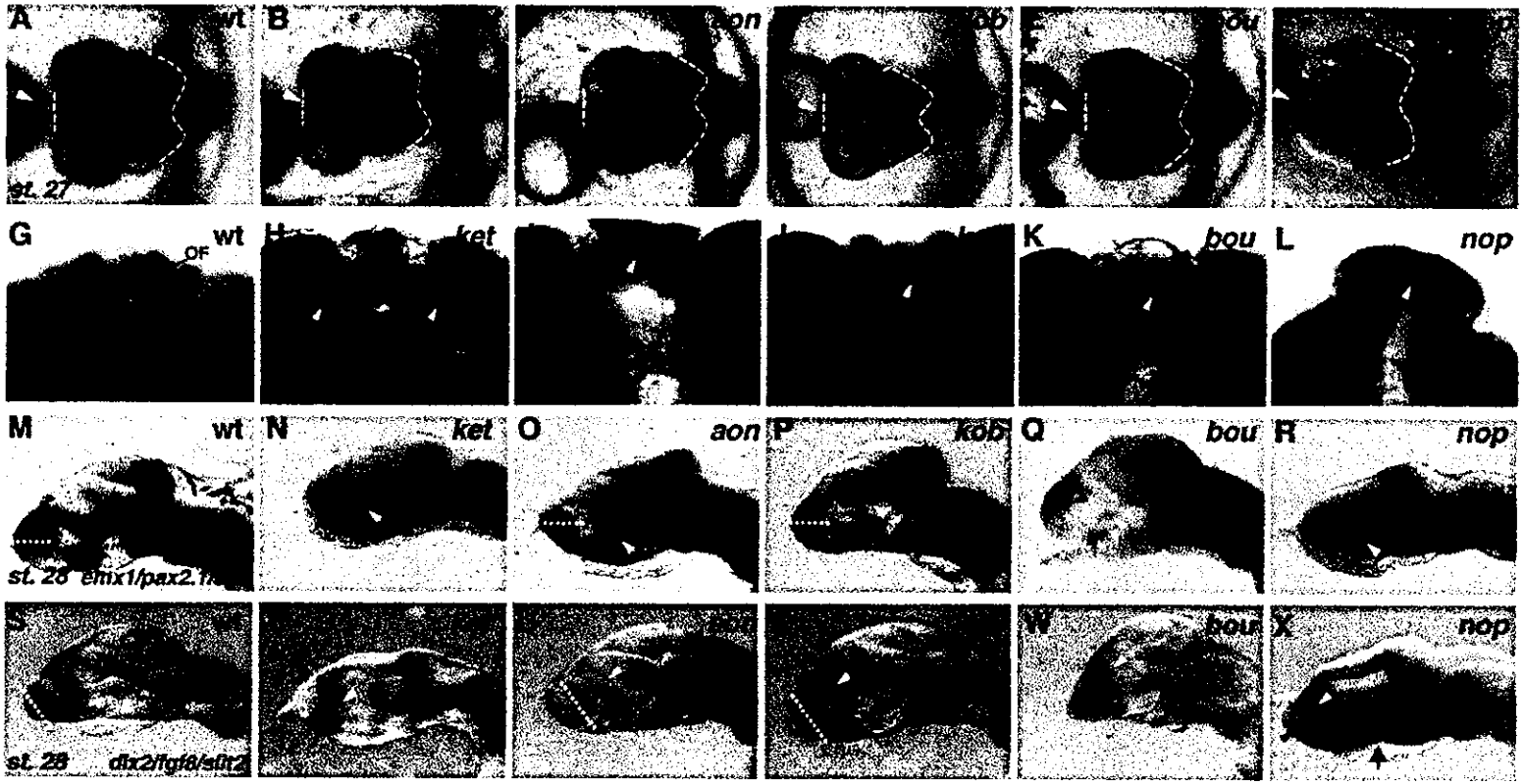

Fig. 2. Class 1 mutant phenotypes. (A,G,M,S) Wild type; (B,H,N,T) *ket*$^{j23\text{-}3B}$; (C,I,O,U) *aon*$^{j9\text{-}2F}$; (D,J,P,V) *kob*$^{j35\text{-}6D}$; (E,K,Q,W) *bou*$^{f118\text{-}2A}$; (F,L,R,X) *nop*$^{j80\text{-}19B}$ embryos. (A–F) Phenotypes of live Class 1 mutant embryos at st. 27 (dorsal view). White and black arrowheads indicate the positions of the telencephalon and midbrain, respectively. All Class 1 mutants show a reduction in the size of the telencephalon. Broken lines indicate the posterior edges of the telencephalon and the midbrain. (G–L) Whole-mount immuno-staining with anti-acetylated-tubulin and anti-HNK antibodies of embryos at st. 31. Ventral view of the anterior portion of the head. AC, anterior commissure; SOT, supraoptic tract; OF, olfactory nerve; ON, optic nerve. (M–X) In situ hybridization analysis of the forebrain of embryos at st 28. Lateral view of the head. (M–R) *emx1/pax2.1/shh*, and (S–X) *dlx2/fgf8/slit2* as probes, respectively.

the *dlx2* expression in the ventral telencephalon was almost absent (black arrowheads in Fig. 2T,X). In these mutants, the *shh* expression along the floor of the diencephalon (white arrowheads in Fig. 2N,R) dorsally expanded and, in *ket* mutant embryos, the expression in the zona limitans intrathalamica (zli) was lost (asterisk in Fig. 2N). The *dlx2* expression in the ventral thalamus showed an anterior shift (white arrowhead in Fig. 2T). In *nop* mutants, the *dlx2* expression marking the ventral thalamus anteriorly shifted, which was accompanied by the anterior expansion of the *dlx2* expression in the pharyngeal arch region (arrow in Fig. 2X).

In *aon* mutant embryos, the *emx1* expression shifted ventrally (broken line in Fig. 2M,O). Concomitantly, two domains of the *dlx2* expression in the ventral telencephalon and ventral thalamus shifted posteriorly (broken line in Fig. 2S,U to show the anterior limit of the *dlx2* expression; black and white arrowheads in Fig. 2U). The anteroventral region of the diencephalic *shh* expression was reduced (white arrowhead in Fig. 2O) and the *shh* expression in the zli was abolished (asterisk in Fig. 2O).

In *kob* mutants, the *emx1* expression shifted ventrally (broken line in Fig. 2P) and the *dlx2* expression in the ventral telencephalon shifted posteriorly (broken line and black arrowhead in Fig. 2V), and the *dlx2* expression in the ventral thalamus decreased (white arrowhead in Fig. 2V). *shh* expression in the zli and ventral diencephalon was low (asterisk and white arrowhead in Fig. 2P, respectively).

In *bou* mutant embryos, the *emx1* expression domain seems compressed anteroposteriorly (black arrowhead in Fig. 2Q) and the *dlx2* expression in the ventral thalamus became noncontinuous (white arrow head in Fig. 2W). The *shh* expression in the diencephalon was only rudimentary (white arrowhead in Fig. 2Q).

Thus, different patterning defects in the forebrain are included in these Class 1 mutants with smaller telencephalon. It is important to note that the majority of the mutants of this Class had an altered *shh* expression, particularly a reduction of *shh* expression in the zli.

2.3.2. Class 1A mutant kentoku representing an early fuction in telencephalon development

The expression of an early telencephalic marker *bf1* (Tao and Lai, 1992) was examined in all the Class 1 mutants. In wild-type Medaka embryos, *bf1* expression becomes detectable in the most anterior region of the brain at st. 19. *ket* mutant at st. 20 uniquely lacked the *bf1* expression (Fig. 3A,B). This observation indicated that *ket* is required in an early step in telencephalon development, possibly in the induction process. In *nop* mutant embryos, *bf1* expression was reduced at st. 20 probably due to the expansion of the diencephalon and mesencephalon at the expense of the telencephalon. In the rest of Class 1 mutants, *bf1* expression appeared normal (data not shown).

2.3.3. Class 1C mutation affecting maintenance of the telencephalon

In *hannya* ($han^{141\text{-}3B}$) mutant embryos, the distance between the eyes decreased (arrow in Fig. 4A,E), but the floor plate was normal (data not shown), ruling out general midline defects. The expression of dorsal *emx1* was reduced in *han* mutant embryos (arrowheads in Fig. 4D,H). The projection pattern of trigeminal nerves was altered such that they did not extend toward the ventral surface of the forebrain at st. 31 (arrowheads in Fig. 4B,C,F,G). By contrast, the anterior commissure appeared normal. This phenotype was unique to *han* mutants and distinguished them from other Class 1 mutants.

2.3.4. Class 1D mutations exhibiting the phenotype similar to that of oep in zebrafish

The mutants of *akatsuki* ($aku^{122\text{-}15A}$), *akebono*($ake^{154\text{-}7A}$) and *mochizuki*($moc^{196\text{-}11B}$), classified to 1D all displayed a drastic morphological phenotype similar to that of *one-eyed-pinhead* (*oep*) in zebrafish (Fig. 5A–D), where only one median eye was formed and the ventral brain tissue was severely affected. This phenotype was very similar to that of the zebrafish *oep* mutant (Schier et al., 1996). These three Medaka mutations sharing similar forebrain phenotypes complemented each other.

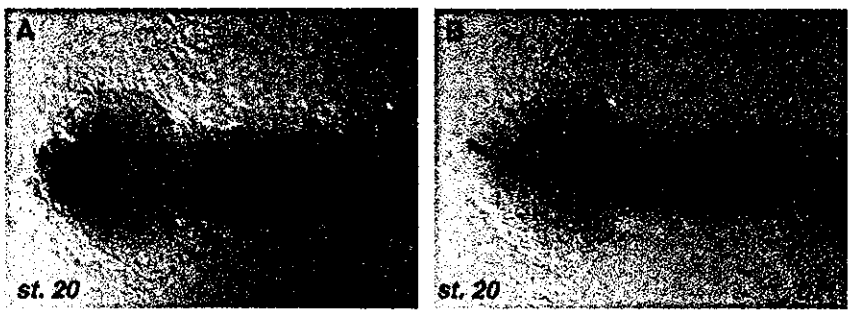

Fig. 3. Loss of *bf1* expression in $ket^{123\text{-}3B}$ mutant embryo at st. 20. (A,B) Whole-mount in situ hybridization analysis of embryos at st. 20 with *bf1* probe. (A) Wild-type embryo. (B) *ket* mutant embryo.

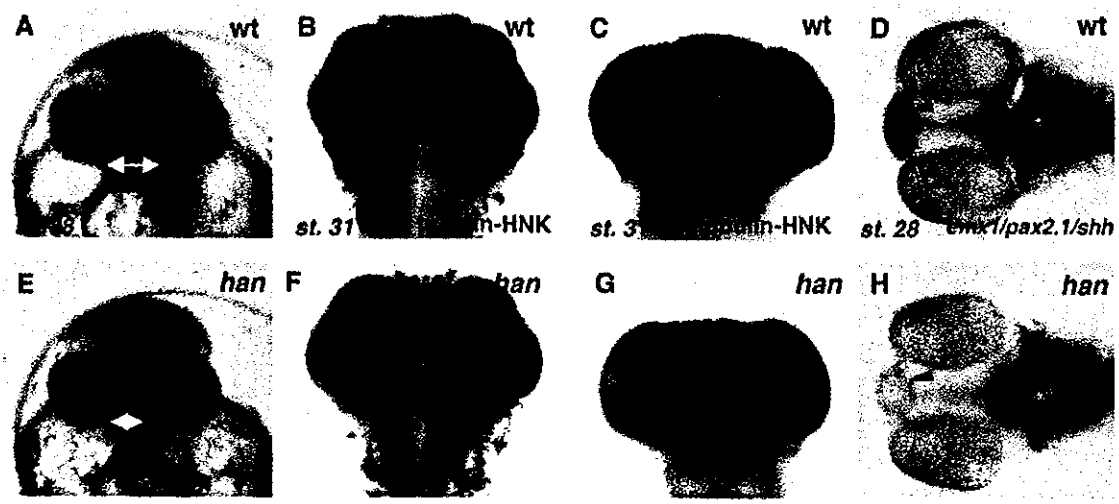

Fig. 4. *han*$^{H1\text{-}3B}$ mutant phenotypes. (A–D) wild type. (E–H) *han* mutant. (A,E) Live phenotype of embryos at st. 33. Anterior front view. Arrows show the width of the telencephalon. (B,C,F,G) Whole-mount staining of embryos at st. 31 with anti-acetylated-tubulin and HNK antibodies. (B,F) Ventral view; (C,G) Anterior front view. Arrowheads show the position of the trigeminal nerve. (D,H) Whole-mount in situ hybridization with *emx1/pax2.1/shh* probe mixture. Dorsal view of embryos at st. 28.

2.4. Class 2 mutations affecting the morphology of the forebrain

Class 2 mutations affecting forebrain shape without altering telencephalon size was divided into the subclasses, 2A to 2C, based on other associated phenotypes (Tables 1 and 2).

2.4.1. Class 2A mutations affecting the forebrain ventricle

We have identified mutations in 6 genes affecting the formation of the forebrain ventricle. In *sarudahiko* (*sar*$^{J106\text{-}4A}$) and *tengu* (*ten*$^{Jr10\text{-}4D}$) mutant embryos, the ventricle of the forebrain did not inflate (arrowheads in Fig. 6A–C), the *emx1* expression did not extend ventrally as in the wild type (black arrowheads in Fig. 6P–R), while the *dlx2* expression remained normal (data not shown). It is remarkable that the *shh* expression in either the brain or the floor plate was absent, suggesting a defect in midline signaling (white arrowheads in Fig. 6Q,R). At the histological level, neuroepithelial cells in the forebrain and cortical layers of the retina were round and did not exhibit the characteristic polarized cell morphology (Fig. 6F–H,K–M). The defect at the cellular level may account for the defect in the histogenesis of the forebrain ventricle in these mutants. *sar* and *ten* mutants also shared a common defect in the cardiovascular system.

In *karuna* (*kar*$^{150\text{-}4A}$) and *oobesshimi* (*oob*$^{J103\text{-}11A}$) mutant embryos, in contrast, the forebrain ventricle was abnormally expanded (arrowheads in Fig. 6A,D–F,I,J). *kar* mutant embryos also had small eyes (Fig. 6D,I), and a forebrain ventricle open on the ventral side (open arrowhead in Fig. 6I). The *shh* expression in the diencephalon was altered in *kar* mutant embryos (white and black arrowheads in Fig. 6S), suggesting that the patterning of the ventral forebrain is affected. In addition, the bilateral retinas were not completely separated in the midline (black arrowhead in Fig. 6I). It is interesting to determine whether this is caused by the altered development of the optic stalk or by a defect in the morphogenetic movement of diencephalon to split

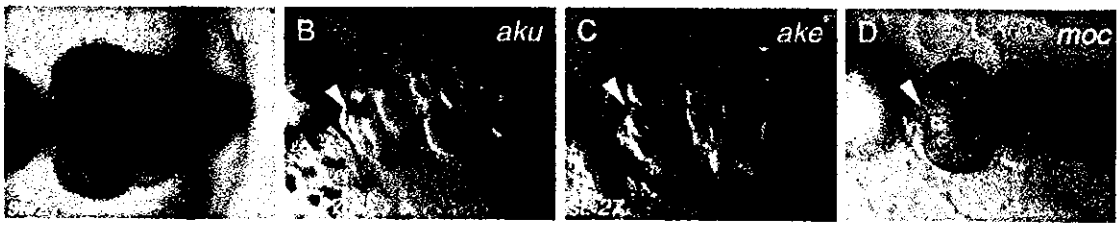

Fig. 5. Mutants in 3 genes display phenotypes similar to that of *oep* zebrafish mutants. (A–D) Dorsal view of st. 27 live embryos of (A) wild-type; (B) *aku*$^{J22\text{-}15A}$ mutant; (C) *ake*$^{J54\text{-}7A}$ mutant and (D) *moc*$^{J96\text{-}11B}$ mutant.

Table 2
Defects in the axonal scaffolds and the gene expressions in the forebrain

Class	Genes	Structures									
		Anti-tubulin + HNK-1				*Emx1*	*Dlx2*		*Shh*		
		AC	SOT	OF	ON	dTel	vTel	vTha	Zli	vFor	Hth
Class 1A	*ket*	def	−	+	+	r	−	as	−	dve	ape
Class 1B	*aon*	def	−	−	+	vs	ps and r	ps and r	−	+	r
	kob	+	+	def	+	ve	ps and r	ps and r	r	r	+
	bou	def	−	def	def	apr	+	f	f	f	f
	nop	nj	nj	−	nj	r	−	as	−	+	pe
Class 2A	*sar*	nd	nd	nd	nd	de and vr	+	+	−	−	−
	ten	+	+	+	r	vr	+	+	−	−	−
	kar	nd	nd	nd	nd	ve	ps	ps and ve	+	+	r
	oob	nd	nd	nd	nd	+	ps and vr	ps and vr	r	r	r

AC, anterior commissure; For, forebrain; Hth, hypothalamus; OF, olfactory nerve; ON, optic nerve; SOT, supraoptic tract; Tel, telencephalon; Tha, thalamus; Zli, zona limitans intrathalamica; +, less affected; −, missing; r, reduced; e, expanded; s, shifted; f, fragmented; def, defasciculated; nj, not judgeable; nd, not done; a, anteriorly; p, posteriorly; d, dorsally; v, ventrally.

a single retinal field into bilateral optic primordia (Varga et al., 1999).

In *oob* mutant embryos, the enlarged ventricle could be observed from st. 25. The roof layer of the telencephalon appeared to be absent and the telencephalon became swollen at later stages (arrowhead in Fig. 6J). Despite the malformation of the forebrain ventricle, the cells in the neuroepithelium were normally polarized (Fig. 6J,O), and

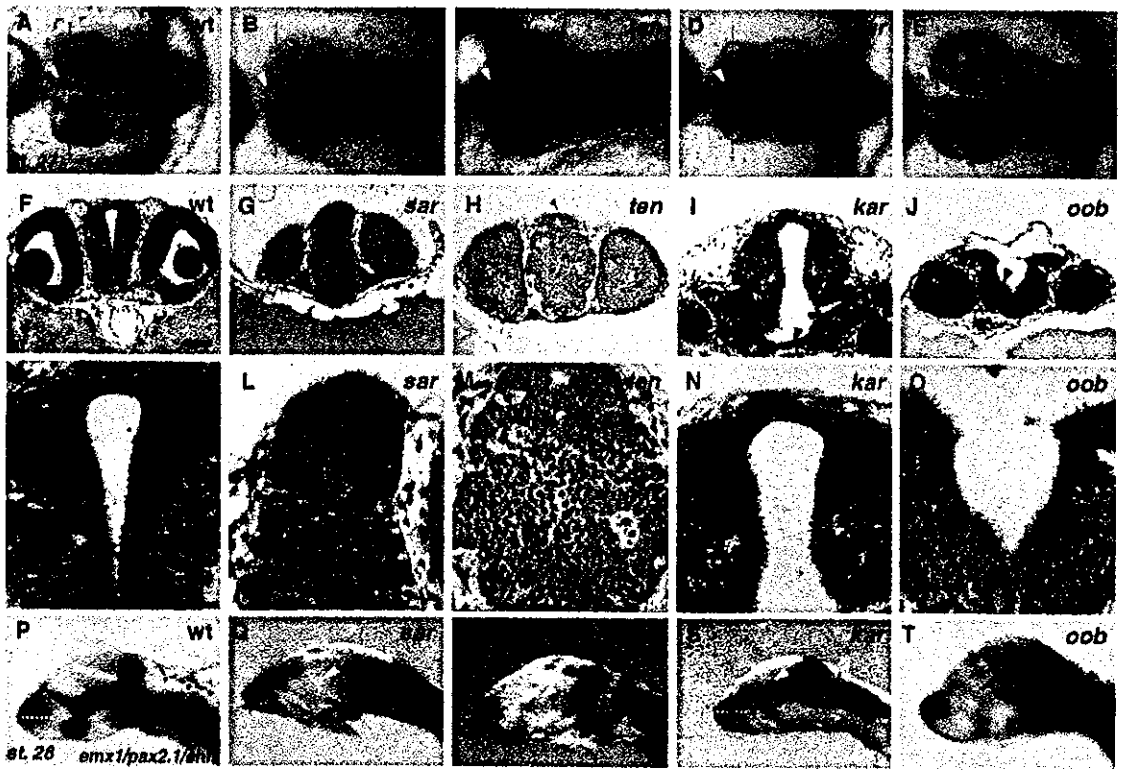

Fig. 6. Class 2A mutant phenotypes. (A,F,K,P) Wild type; (B,G,L,Q) $sar^{j106\text{-}4A}$; (C,H,M,R) $ten^{jr10\text{-}4D}$; (D,I,N,S) $kar^{j50\text{-}4A}$; (E,J,O,T) $oob^{j103\text{-}11A}$ embryos. (A–E) Live phenotypes of Class 2A mutant embryos at st. 27 (dorsal view). Arrowheads show the forebrain ventricle. (F–J) Transverse sections of embryos at st. 26, stained with hematoxylin and eosin. (K–O) A higher magnification image of the transverse sections, focused on the cell layers around the forebrain ventricle. (P–T) Whole-mount in situ hybridization analysis of embryos at st. 28 with *emx1/pax2.1/shh* probe mixture. Lateral view of the brain. Scale bar, 50 μm.

the general pattern of gene expression was not significantly affected, except for the reduction in *shh* expression in the diencephalon (arrowhead in Fig. 6T).

2.4.2. Class 2B mutations affecting formation of anterior commissure

Anterior commissure nerves connect the two telencephalic hemispheres. We have identified two genes required for the formation of the commissure of bilateral axons from the dorsal telencephalon (Class 2B mutants).

In *shikami* (*shi*$^{j92\text{-}3A}$) mutant embryos, axons from the bilateral telencephalic halves did not associate with each other at the midline (arrowhead in Fig. 7D). Interestingly, it appears that axons originating from one side of the telencephalon crossed once to the other side then returned to the midline. The telencephalon tended to be distorted in *shi* mutant embryos (arrowhead in Fig. 7C).

In *ikazuchi* (*ika*$^{j94\text{-}8A}$) mutant embryos, axons from telencephalic clusters defasciculated and formed ectopic minor commissures in the dorsal telencephalon (arrowhead in Fig. 7F). The forebrain of *ika* was slightly enlarged (arrowhead in Fig. 7E).

2.4.3. The baltan mutation of Class 2D with a unique set of forebrain defects

baltan (*bal*$^{j102\text{-}2A}$) mutant embryos were recognized by an early focal neural degeneration in the forebrain, leading to a reduction of the forebrain size and an edema (Fig. 8A,G). Surprisingly, staining of axons of cranial nerves revealed that many axons crossed the midline at various A–P levels, causing a ladderlike appearance (arrowheads in Fig. 8B,H). The bilateral optic nerve did not form a chiasm between the eyes but crossed the midline at the anterior commissure (arrowheads in Fig. 8C,I). The *emx1* expression was absent and the *dlx2* expression in the ventral telencephalon was attenuated (black arrowheads in Fig. 8D,E,J,K). *dlx2* expression in the ventral thalamus was markedly reduced (white arrowheads in Fig. 8E,K), suggesting a seriously defective regionalization of the forebrain in the *baltan*

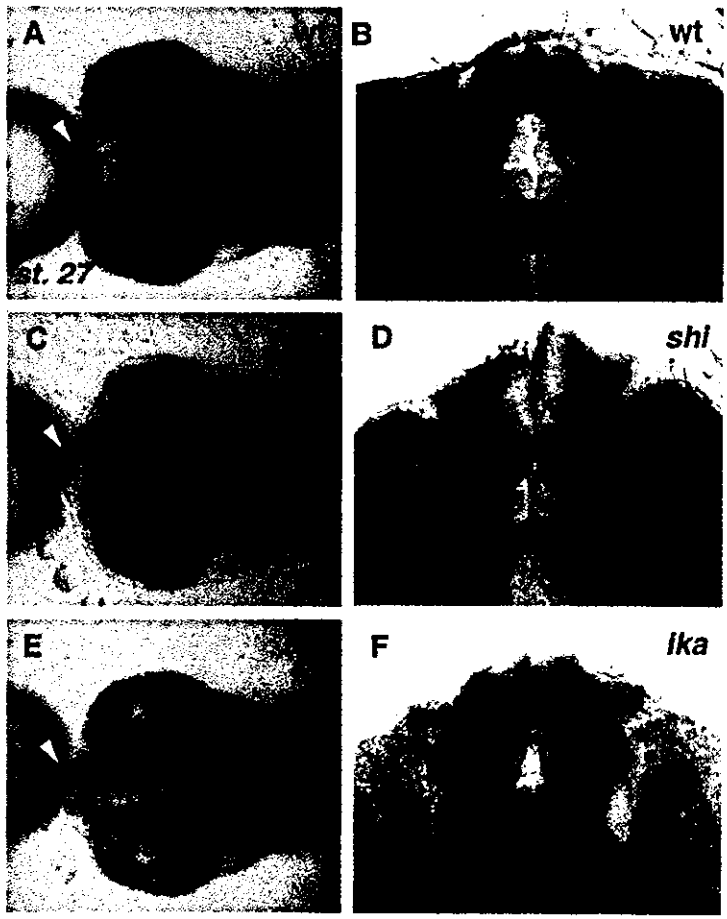

Fig. 7. Class 2B mutant phenotypes. (A,B) wild type; (C,D) *shi*$^{j92\text{-}3A}$; (E,F) *ika*$^{j94\text{-}8A}$. (A,C,E) Morphology of Class 2B mutant embryos at st. 27 (dorsal view). (B,D,F) Whole-mount staining of embryos at st. 31 with anti-acetylated-tubulin and HNK antibodies. Arrowheads show the anterior commissure.

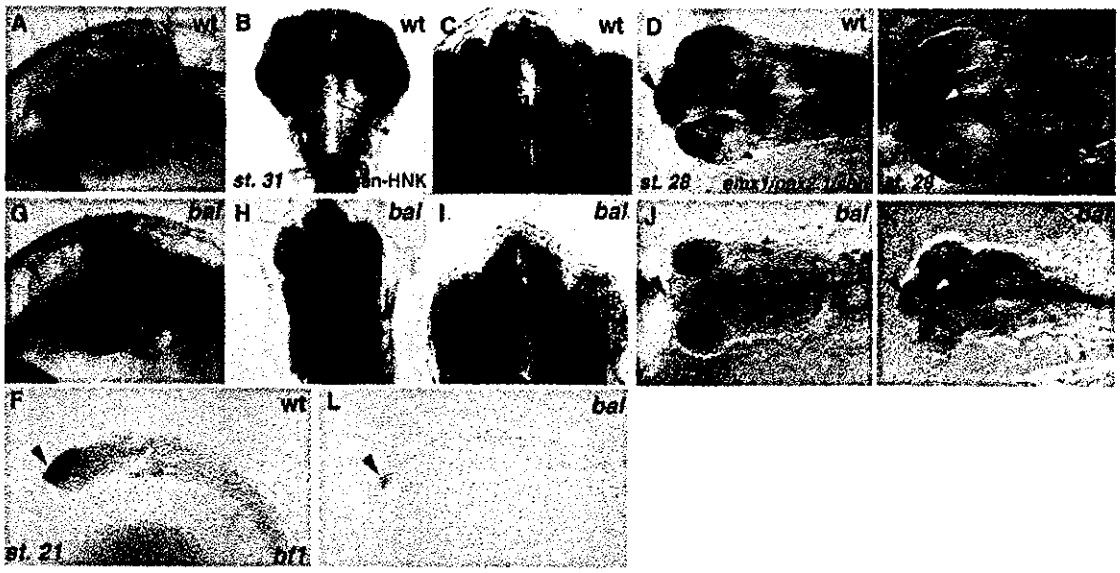

Fig. 8. $bal^{102\text{-}2A}$ mutant phenotypes. (A–F) Wild type; (G–L) $bal^{102\text{-}2A}$ embryos. (A,G) Live embryos of wild-type (A) and (G) $bal^{102\text{-}2A}$ mutant at st. 30 (lateral view). An arrowhead in G shows an empty space generated by degeneration in the forebrain. (B,C,H,I) Whole-mount immunostaining of st. 31 embryos using anti-acetylated tubulin and HNK antibodies. (B,H) Ventral view of the head. An arrowhead indicates ladder like axons of unknown origin. (C,I) enlarged view of (B,H). an arrowhead shows the optic nerve. (D–F,J–L) Whole-mount in situ hybridization analysis of embryos at st.28 (D,E,J,K, dorsal view) and st.21 (F,L, lateral view), using (D,J) *emx1/pax2.1/shh*; (E,K) *dlx2/fgf8/slit2* and (F,L) *bf1* as probes. (F,L) Arrowheads indicate the *bf1* expression in the telencephalon.

mutant. Moreover, *bf1* expression at the induction phase of telencephalon was remarkably reduced (Fig. 8F,L). These results suggested that *bal* is necessary for early specification of the forebrain as well as proper axonal projection of cranial nerves.

3. Discussion

3.1. Class 1 mutations causing smaller telencephalon

ket mutants are remarkable for their compromised expression of the early telencephalon marker *bf1*(Fig. 3). In parallel, both *emx1* expression in the dorsal telencephalon and the *dlx2* expression in the ventral telencephalon are strongly reduced, raising the possibility that *ket* is a key regulator required for specification of the telencephalon (Fig. 2N,T). The phenotype of *ket* mutants is reminiscent of that of the *bf1* knockout mouse with hypoplasia of the cerebral hemispheres and more severe defects in the basal region of the telencephalon (Dou et al., 1999). The expression of both *bf1* and *emx1* is reduced in *tlc*- knockdown embryos after the injection of antisense morpholino oligonucleotides (Houart et al., 2002). The possible genetic linkage of *ket* with *bf1* and *tlc* is currently under investigation. In mice, Fgf8 induces *bf1* expression under in vitro culture condition of the forebrain tissue (Shimamura and Rubenstein, 1997). However, telencephalon is somehow formed in the *fgf8* mutants of mice and zebrafish, suggesting it alone is not responsible for induction of the telencephalon (Meyers et al., 1998; Reifers et al., 1998; Shanmugalingam et al., 2000; Shinya et al., 2001).

The major feature of *aon* and *kob* mutants is their defect in dorsoventral (D–V) patterning in the telencephalon. The tissue area for *emx1* expression in the dorsal telencephalon expands or shifts ventrally, and the *dlx2* expression in the ventral telencephalon is reduced and posteriorly displaced (Fig. 2O,P,U,V).

shh-null mice lack any signs of the medial ganglionic eminence (MGE), which is the ventral portion of the basal ganglia, indicating that Shh is required for the patterning of the ventral telencephalon (Chiang et al., 1996). However, it is yet to be determined which part of *shh* expression in the forebrain is required for the D–V patterning of the telencephalon. All the Class 1 mutants have an altered *shh* expression, particularly in the zli (Fig. 2N–R). The zli not only forms a clear histological border between the dorsal and ventral thalami (Larsen et al., 2001), but, for its *shh* expression, is considered to function as a secondary organizing center. The presence of patterning defects of the telencephalon in Class 2 mutants corroborates this notion.

It is to be noted that the phenotype of the Class 1 mutants associated with the decreased expression of *shh* in the forebrain does not resemble those of zebrafish mutants defective in sonic hedgehog signaling, *sonic you* (*syu*),

detour (*dtr*), *you-too* (*yot*) and *slow-muscle-omitted* (*smu*), in which *shh*, *gli1*, *gli2*, *foxh1* and *smoothened*, respectively, are mutated and the primary causes are defects in the midline tissues (Schauerte et al., 1998; Karlstrom et al., 1999; Barresi et al., 2000; Chen et al., 2001; Varga et al., 2001; Karlstrom et al., 2003).

The phenotype of the *nop* mutant, characterized by the expansion of the diencephalon and mesencephalon at the expense of the telencephalon tissue (Fig. 2F), is reminiscent of those of *masterblind(mbl)* and *headless* (*hdl*) mutants of zebrafish. In these zebrafish mutants, the genes coding for the negative regulators of Wnt signaling, *tcf3* and *axin1*, respectively, are mutated, possibly resulting in the over-activation of Wnt signaling throughout the forebrain (Kim et al., 2000; Heisenberg et al., 2001). It is also known that a secreted Wnt antagonist *tlc* is expressed in the anterior neural ridge (Houart et al., 2002). Whether the *nop* gene function is involved in Wnt signaling is of an immediate interest.

3.2. Patterning defects resulting in defective formation of forebrain ventricle

sar and *ten* mutants lack polarized cell shape in the neuroepithelium on one hand (Fig. 6L,M), and show an attenuated *shh* expression in the forebrain and spinal cord on the other (Fig. 6Q,R). It is currently under investigation how these phenotypes correlate with each other.

In *oob* mutants showing the expansion of the forebrain ventricle, the roof plate is missing and the basal plate is thicker (Fig. 6J). This phenotype may reflect an altered D–V patterning or a defect in the histogenetic process dependent on cell–cell interactions. It is interesting to note that the phenotype of *oob* mutants somewhat resembles that of the zebrafish *parachute* mutant of the N-cadherin gene (Lele et al., 2002; Erdmann et al., 2003).

3.3. Mutations affecting axonal paths in the forebrain

Class 2B mutants have characteristic defects in the formation of the anterior commissure. Interestingly, the formation of the anterior commissure is affected differently in *shi* and *ika* mutants, suggesting that *shi* and *ika* may be required for a distinct process in anterior commissure formation (Fig. 7).

It is suggested in zebrafish that a commissure is formed through three steps (Bak and Fraser, 2003). The first step is the extension of the leader axon toward the midline through the already defined axonal tract. The growth cone senses and integrates attractive and repulsive midline cues for their behavior. The second step is the growth and extension of the follower axon along the leader axon toward the midline and its fasciculation with the leader axon. The third step is the interaction of the axons with the leader axon of the opposite side across the midline and mutual fasciculation. In this way, the leader axons from two sides cooperate with each other to establish a commisure across the midline.

In *ika* mutants, the first step may be disturbed since the anterior commisure was formed but in an ectopic position (Fig. 7F). The group of Class 1 mutants, *bou*, *ket* and *aon*, may have a defect in the second step. The failure of the axons to properly cross the midline in *bou* mutants may be explained by the loss of interaction between the leader and follower axons (Fig. 2K). In *ket* and *aon* mutants, a mild defasciculation of axons in the anterior commissure was observed (Fig. 2H,I).

In *bal* mutants, the anterior commissure and optic nerve joined together. In the region between the anterior commissure and the optic nerve, Netrins, the repulsive cues for axons, are known to be expressed. Indeed, the *netrin* expression in this region was altered in *noi* and *ace* zebrafish mutant embryos, accompanied by abnormalities of the anterior and postoptic commissures (Macdonald et al., 1997; Shanmugalingam et al., 2000). It would be interesting to determine whether the *netrin* expression between the anterior commissure and the optic nerve is altered in *bal* mutants. In *shi* mutants, the third step may be affected, since the commissure structure crossing the midline was not established.

In the Class 1 mutants which have altered gene expression pattern, the formation of axonal scaffolds in the forebrain is also affected, as summarized in Table 2. In zebrafish, the boundaries of regulatory gene expression domains correspond in many cases to early axonal scaffolds in the forebrain (Macdonald et al., 1994). It has been hypothesized that a growth cone extends along the interface between two domains of cells with different cell surface properties. Class 1 Medaka mutants should prove useful in testing this hypothesis.

3.4. Medaka and zebrafish complement to genetically dissect forebrain formation

We have identified 25 loci required for the formation of the forebrain in the systematic screen in Medaka. Although screenings covering the whole genome have already been carried out in zebrafish, we identified a battery of mutations resulting in phenotypes that were not observed in the zebrafish mutant collection. This could reflect (1) the difference in the functional overlap of genes, (2) the difference in the regulation of forebrain development, (3) the difference in susceptibility to mutagens of a genetic locus between Medaka and zebrafish.

Some other mutant phenotypes corresponded to those of identified zebrafish mutants. These mutated genes of shared phenotypes must be involved in the genetic pathways conserved between the two species. Interestingly, mutations in 3 genes, *aku*, *ake* and *moc* of Class 1D result in a phenotype similar to that of *one-eyed-pinhead* (*oep*) in zebrafish (Schier et al., 1997; Strahle et al., 1997). In zebrafish, mutants of other genes involved in Nodal

signaling, *cyclops(cyc)*, *squint* (*sqt*), and *schmalspur* (*sur*) displayed slightly different phenotypes, suggesting a divergence of the molecular components in a signaling pathway between the two species (Hatta et al., 1994; Brand et al., 1996b; Malicki et al., 1996; Schier et al., 1996; Heisenberg and Nusslein-Volhard, 1997; Feldman et al., 1998; Rebagliati et al., 1998; Sampath et al., 1998; Pogoda et al., 2000; Sirotkin et al., 2000). Similarly, mutations in 3 genes, *oob*, *sam*, and *sgu*, caused phenotypes that are reminiscent of those of *parachute* zebrafish mutant of the N-cadherin gene. No mutations in other genes are reported in zebrafish to cause the *parachute* phenotype (Lele et al., 2002; Erdmann et al., 2003). Cloning of these mutated genes in Medaka and the analysis of their function will reveal both conserved and divergent functions of the genes essential for forebrain formation. The results of the mutant screen in Medaka do demonstrate that zebrafish and Medaka complement each other in uncovering more genes and more functions involved in the developmental process.

4. Experimental procedures

4.1. Mutant embryos

Fish are mutagenized and screened for mutations as described in an accompanying paper (Furutani-Seiki et al., this issue). Mutant embryos were obtained by mating heterozygotes, reared at 28 °C, and staged according to the development of sibling normal embryos. Live embryos were photographed after removing the chorion and mounting in 2.5% methylcellulose.

4.2. Histological methods

Whole-mount staining of the embryos by in situ hybridization or with anti-acetylated tubulin/anti-HNK1 antibodies was performed as described by Hammerschmidt and Nusslein-Volhard (1993). RNA probes for in situ hybridization were labeled with digoxygenin, and detected using an anti-digoxygenin antibody conjugated with alkalinephophatase, and reacted with BM purple (Roche) for color development. For histological sections, the embryos were fixed in 4% paraformaldehyde, dehydrated through ethanol series and embedded in Jung HistoResin Plus (Leica) and sections 4 μm thickness of were made.

Acknowledgements

We are grateful to Dr Giselbert Hauptmann for input about regionalization of medaka brain, Drs Takashi Sasaki and Noboru Nakajima for cloning *slit2*, *dlx2* and *bf1* probes. This work was supported by the ERATO project of the Japan Science and Technology Agency to H.K.

References

Bak, M., Fraser, S.E., 2003. Axon fasciculation and differences in midline kinetics between pioneer and follower axons within commissural fascicles. Development 130, 4999–5008.

Barresi, M.J., Stickney, H.L., Devoto, S.H., 2000. The zebrafish slow-muscle-omitted gene product is required for Hedgehog signal transduction and the development of slow muscle identity. Development 127, 2189–2199.

Brand, M., Heisenberg, C.P., Jiang, Y.J., Beuchle, D., Lun, K., Furutani-Seiki, M., et al., 1996a. Mutations in zebrafish genes affecting the formation of the boundary between midbrain and hindbrain. Development 123, 179–190.

Brand, M., Heisenberg, C.P., Warga, R.M., Pelegri, F., Karlstrom, R.O., Beuchle, D., et al., 1996b. Mutations affecting development of the midline and general body shape during zebrafish embryogenesis. Development 123, 129–142.

Bulfone, A., Puelles, L., Porteus, M.H., Frohman, M.A., Martin, G.R., Rubenstein, J.L., 1993. Spatially restricted expression of Dlx-1, Dlx-2 (Tes-1), Gbx-2, and Wnt-3 in the embryonic day 12.5 mouse forebrain defines potential transverse and longitudinal segmental boundaries. J. Neurosci. 13, 3155–3172.

Chen, W., Burgess, S., Hopkins, N., 2001. Analysis of the zebrafish smoothened mutant reveals conserved and divergent functions of hedgehog activity. Development 128, 2385–2396.

Chiang, C., Litingtung, Y., Lee, E., Young, K.E., Corden, J.L., Westphal, H., Beachy, P.A., 1996. Cyclopia and defective axial patterning in mice lacking Sonic hedgehog gene function. Nature 383, 407–413.

Dou, C.L., Li, S., Lai, E., 1999. Dual role of brain factor-1 in regulating growth and patterning of the cerebral hemispheres. Cereb. Cortex 9, 543–550.

Erdmann, B., Kirsch, F.P., Rathjen, F.G., More, M.I., 2003. N-cadherin is essential for retinal lamination in the zebrafish. Dev. Dyn. 226, 570–577.

Feldman, B., Gates, M.A., Egan, E.S., Dougan, S.T., Rennebeck, G., Sirotkin, H.I., et al., 1998. Zebrafish organizer development and germ-layer formation require nodal-related signals. Nature 395, 181–185.

Fernandez, A.S., Pieau, C., Reperant, J., Boncinelli, E., Wassef, M., 1998. Expression of the Emx-1 and Dlx-1 homeobox genes define three molecularly distinct domains in the telencephalon of mouse, chick, turtle and frog embryos: implications for the evolution of telencephalic subdivisions in amniotes. Development 125, 2099–2111.

Figdor, M.C., Stern, C.D., 1993. Segmental organization of embryonic diencephalon. Nature 363, 630–634.

Furutani-Seiki, M., Jiang, Y.J., Brand, M., Heisenberg, C.P., Houart, C., Beuchle, D., et al., 1996. Neural degeneration mutants in the zebrafish, *Danio rerio*. Development 123, 229–239.

Hatta, K., Puschel, A.W., Kimmel, C.B., 1994. Midline signaling in the primordium of the zebrafish anterior central nervous system. Proc. Natl Acad. Sci. USA 91, 2061–2065.

Hauptmann, G., Gerster, T., 2000. Regulatory gene expression patterns reveal transverse and longitudinal subdivisions of the embryonic zebrafish forebrain. Mech. Dev. 91, 105–118.

Hauptmann, G., Soll, I., Gerster, T., 2002. The early embryonic zebrafish forebrain is subdivided into molecularly distinct transverse and longitudinal domains. Brain Res. Bull. 57, 371–375.

Heisenberg, C.P., Nusslein-Volhard, C., 1997. The function of silberblick in the positioning of the eye anlage in the zebrafish embryo. Dev. Biol. 184, 85–94.

Heisenberg, C.P., Brand, M., Jiang, Y.J., Warga, R.M., Beuchle, D., van Eeden, F.J., et al., 1996. Genes involved in forebrain development in the zebrafish, *Danio rerio*. Development 123, 191–203.

Heisenberg, C.P., Houart, C., Take-Uchi, M., Rauch, G.J., Young, N., Coutinho, P., et al., 2001. A mutation in the Gsk3-binding domain of zebrafish Masterblind/Axin1 leads to a fate transformation of telencephalon and eyes to diencephalon. Genes Dev. 15, 1427–1434.

Houart, C., Westerfield, M., Wilson, S.W., 1998. A small population of anterior cells patterns the forebrain during zebrafish gastrulation. Nature 391, 788–792.

Houart, C., Caneparo, L., Heisenberg, C., Barth, K., Take-Uchi, M., Wilson, S., 2002. Establishment of the telencephalon during gastrulation by local antagonism of Wnt signaling. Neuron 35, 255–265.

Ishikawa, Y., Hyodo-Taguchi, Y., 1994. Cranial nerves and brain fiber systems of the medaka fry as observed by a whole-mount staining method. Neurosci. Res. 19, 379–386.

Iwamatsu, T., 1994. Stages of normal development in the medaka *Oryzias latipes*. Zool. Sci. 11, 825–839.

Karlstrom, R.O., Talbot, W.S., Schier, A.F., 1999. Comparative synteny cloning of zebrafish you-too: mutations in the Hedgehog target gli2 affect ventral forebrain patterning. Genes Dev. 13, 388–393.

Karlstrom, R.O., Tyurina, O.V., Kawakami, A., Nishioka, N., Talbot, W.S., Sasaki, H., Schier, A.F., 2003. Genetic analysis of zebrafish gli1 and gli2 reveals divergent requirements for gli genes in vertebrate development. Development 130, 1549–1564.

Kim, C.H., Oda, T., Itoh, M., Jiang, D., Artinger, K.B., Chandrasekharappa, S.C., et al., 2000. Repressor activity of Headless/Tcf3 is essential for vertebrate head formation. Nature 407, 913–916.

Larsen, C.W., Zeltser, L.M., Lumsden, A., 2001. Boundary formation and compartition in the avian diencephalon. J. Neurosci. 21, 4699–4711.

Lele, Z., Folchert, A., Concha, M., Rauch, G.J., Geisler, R., Rosa, F., et al., 2002. parachute/n-cadherin is required for morphogenesis and maintained integrity of the zebrafish neural tube. Development 129, 3281–3294.

Macdonald, R., Xu, Q., Barth, K.A., Mikkola, I., Holder, N., Fjose, A., et al., 1994. Regulatory gene expression boundaries demarcate sites of neuronal differentiation in the embryonic zebrafish forebrain. Neuron 13, 1039–1053.

Macdonald, R., Scholes, J., Strahle, U., Brennan, C., Holder, N., Brand, M., Wilson, S.W., 1997. The Pax protein Noi is required for commissural axon pathway formation in the rostral forebrain. Development 124, 2397–2408.

Malicki, J., Neuhauss, S.C., Schier, A.F., Solnica-Krezel, L., Stemple, D.L., Stainier, D.Y., et al., 1996. Mutations affecting development of the zebrafish retina. Development 123, 263–273.

Mathieu, J., Barth, A., Rosa, F.M., Wilson, S.W., Peyrieras, N., 2002. Distinct and cooperative roles for Nodal and Hedgehog signals during hypothalamic development. Development 129, 3055–3065.

Meyers, E.N., Lewandoski, M., Martin, G.R., 1998. An Fgf8 mutant allelic series generated by Cre- and Flp-mediated recombination. Nat. Genet. 18, 136–141.

Pogoda, H.M., Solnica-Krezel, L., Driever, W., Meyer, D., 2000. The zebrafish forkhead transcription factor FoxH1/Fast1 is a modulator of nodal signaling required for organizer formation. Curr. Biol. 10, 1041–1049.

Puelles, L., Rubenstein, J.L., 1993. Expression patterns of homeobox and other putative regulatory genes in the embryonic mouse forebrain suggest a neuromeric organization. Trends Neurosci. 16, 472–479.

Puelles, L., Kuwana, E., Puelles, E., Bulfone, A., Shimamura, K., Kelcher, J., et al., 2000. Pallial and subpallial derivatives in the embryonic chick and mouse telencephalon, traced by the expression of the genes Dlx-2, Emx-1, Nkx-2.1, Pax-6, and Tbr-1. J. Comp. Neurol. 424, 409–438.

Rallu, M., Corbin, J.G., Fishell, G., 2002. Parsing the prosencephalon. Nat. Rev. Neurosci. 3, 943–951.

Rebagliati, M.R., Toyama, R., Haffter, P., Dawid, I.B., 1998. Cyclops encodes a nodal-related factor involved in midline signaling. Proc. Natl Acad. Sci. USA 95, 9932–9937.

Reifers, F., Bohli, H., Walsh, E.C., Crossley, P.H., Stainier, D.Y., Brand, M., 1998. Fgf8 is mutated in zebrafish acerebellar (ace) mutants and is required for maintenance of midbrain–hindbrain boundary development and somitogenesis. Development 125, 2381–2395.

Rohr, K.B., Barth, K.A., Varga, Z.M., Wilson, S.W., 2001. The nodal pathway acts upstream of hedgehog signaling to specify ventral telencephalic identity. Neuron 29, 341–351.

Sampath, K., Rubinstein, A.L., Cheng, A.M., Liang, J.O., Fekany, K., Solnica-Krezel, L., et al., 1998. Induction of the zebrafish ventral brain and floorplate requires cyclops/nodal signalling. Nature 395, 185–189.

Schauerte, H.E., van Eeden, F.J., Fricke, C., Odenthal, J., Strahle, U., Haffter, P., 1998. Sonic hedgehog is not required for the induction of medial floor plate cells in the zebrafish. Development 125, 2983–2993.

Schier, A.F., Neuhauss, S.C., Harvey, M., Malicki, J., Solnica-Krezel, L., Stainier, D.Y., et al., 1996. Mutations affecting the development of the embryonic zebrafish brain. Development 123, 165–178.

Schier, A.F., Neuhauss, S.C., Helde, K.A., Talbot, W.S., Driever, W., 1997. The one-eyed pinhead gene functions in mesoderm and endoderm formation in zebrafish and interacts with no tail. Development 124, 327–342.

Shanmugalingam, S., Houart, C., Picker, A., Reifers, F., Macdonald, R., Barth, A., et al., 2000. Ace/Fgf8 is required for forebrain commissure formation and patterning of the telencephalon. Development 127, 2549–2561.

Shimamura, K., Rubenstein, J.L., 1997. Inductive interactions direct early regionalization of the mouse forebrain. Development 124, 2709–2718.

Shinya, M., Koshida, S., Sawada, A., Kuroiwa, A., Takeda, H., 2001. Fgf signalling through MAPK cascade is required for development of the subpallial telencephalon in zebrafish embryos. Development 128, 4153–4164.

Sirotkin, H.I., Gates, M.A., Kelly, P.D., Schier, A.F., Talbot, W.S., 2000. Fast1 is required for the development of dorsal axial structures in zebrafish. Curr. Biol. 10, 1051–1054.

Strahle, U., Jesuthasan, S., Blader, P., Garcia-Villalba, P., Hatta, K., Ingham, P.W., 1997. One-eyed pinhead is required for development of the ventral midline of the zebrafish (*Danio rerio*) neural tube. Genes Funct. 1, 131–148.

Tao, W., Lai, E., 1992. Telencephalon-restricted expression of BF-1, a new member of the HNF-3/fork head gene family, in the developing rat brain. Neuron 8, 957–966.

Varga, Z.M., Wegner, J., Westerfield, M., 1999. Anterior movement of ventral diencephalic precursors separates the primordial eye field in the neural plate and requires cyclops. Development 126, 5533–5546.

Varga, Z.M., Amores, A., Lewis, K.E., Yan, Y.L., Postlethwait, J.H., Eisen, J.S., Westerfield, M., 2001. Zebrafish smoothened functions in ventral neural tube specification and axon tract formation. Development 128, 3497–3509.

Wilson, S.W., Rubenstein, J.L., 2000. Induction and dorsoventral patterning of the telencephalon. Neuron 28, 641–651.

ELSEVIER

Mechanisms of Development 121 (2004) 791–802

www.elsevier.com/locate/modo

Research paper

Mutations affecting liver development and function in Medaka, *Oryzias latipes*, screened by multiple criteria

Tomomi Watanabe[a], Satoshi Asaka[a], Daiju Kitagawa[a], Kota Saito[a], Ryumei Kurashige[a], Takao Sasado[b], Chikako Morinaga[b], Hiroshi Suwa[b], Katsutoshi Niwa[b], Thorsten Henrich[b], Yukihiro Hirose[c], Akihito Yasuoka[d], Hiroki Yoda[e], Tomonori Deguchi[e], Norimasa Iwanami[f], Sanae Kunimatsu[f], Masakazu Osakada[e], Felix Loosli[h], Rebecca Quiring[h], Matthias Carl[h], Clemens Grabher[h], Sylke Winkler[h], Filippo Del Bene[h], Joachim Wittbrodt[h], Keiko Abe[d], Yousuke Takahama[f], Katsuhito Takahashi[g], Toshiaki Katada[a], Hiroshi Nishina[a,*], Hisato Kondoh[b], Makoto Furutani-Seiki[b,*]

[a]*Department of Physiological Chemistry, Graduate School of Pharmaceutical Sciences, University of Tokyo, Tokyo 113-0033, Japan*
[b]*ERATO, Jaman Science and Technology Corporation, Kondoh Differentiation Signaling Project, Kawara-cho 14, Yoshida, Sakyo-ku, Kyoto 606-8305, Japan*
[c]*Graduate School of Biostudies, Kyoto University, Kyoto 606-8501, Japan*
[d]*Department of Applied Biological Chemistry, University of Tokyo, Tokyo 113-0033, Japan*
[e]*Graduate School of Frontier Biosciences, Osaka University, Osaka 565-0871, Japan*
[f]*Division of Experimental Immunology, Institute for Genome Research, The University of Tokushima, Tokushima 770-8503, Japan*
[g]*Department of Molecular Medicine and Pathophysiology, Research Institute, Osaka Medical Center for Cancer and Cardiovascular Diseases, Osaka 537-8511, Japan*
[h]*Developmental Biology Programme, EMBL Heidelberg, Meyerhofstrasse 1, D-69117, Heidelberg, Germany*

Received 20 January 2004; received in revised form 30 March 2004; accepted 3 April 2004

Abstract

We report here mutations affecting various aspects of liver development and function identified by multiple assays in a systematic mutagenesis screen in Medaka. The 22 identified recessive mutations assigned to 19 complementation groups fell into five phenotypic groups. Group 1, showing defective liver morphogenesis, comprises mutations in four genes, which may be involved in the regulation of growth or patterning of the gut endoderm. Group 2 comprises mutations in three genes that affect the laterality of the liver; in *kendama* mutants of this group, the laterality of the heart and liver is uncoupled and randomized. Group 3 includes mutations in three genes altering bile color, indicative of defects in hemoglobin–bilirubin metabolism and *globin* synthesis. Group 4 consists of mutations in three genes, characterized by a decrease in the accumulation of fluorescent metabolite of a phospholipase A_2 substrate, PED6, in the gall bladder. Lipid metabolism or the transport of lipid metabolites may be affected by these mutations. Mutations in Groups 3 and 4 may provide animal models for relevant human diseases. Group 5 mutations in six genes affect the formation of endoderm, endodermal rods and hepatic bud from which the liver develops. These Medaka mutations, identified by morphological and metabolite marker screens, should provide clues to understanding molecular mechanisms underlying formation of a functional liver.

Keywords: Liver development; Medaka; Hepatoblast; Hepatic bud; Laterality; Gall bladder; Lipid metabolism; Endoderm formation; Bile; Zebrafish

1. Introduction

The liver is an organ with vital functions, including processing and storage of nutrients, maintenance of serum composition, detoxification and bile production. The major functional cells of a liver are the hepatocytes

* Corresponding authors. Tel.: +81-75-771-9362; fax: +81-75-771-3835 (M. Furutani-Seiki); Tel.: +81-3-5841-4754; fax: +81-3-5841-4751 (H. Nishina).
E-mail addresses: furutani@dsp.jst.go.jp (M. Furutani-Seiki), nishina@mol.f.u-tokyo.ac.jp (H. Nishina).

0925-4773/$ - see front matter © 2004 Elsevier Ireland Ltd. All rights reserved.
doi:10.1016/j.mod.2004.04.004